

Spin transfer torques generated by the anomalous Hall effect and anisotropic magnetoresistance.

Tomohiro Taniguchi

*National Institute of Advanced Industrial Science and Technology (AIST),
Spintronics Research Center, Tsukuba, Ibaraki 305-8568, Japan and
Center for Nanoscale Science and Technology, National Institute of
Standards and Technology, Gaithersburg, Maryland 20899-6202, USA*

J. Grollier

Unité Mixte de Physique CNRS/Thales and Université Paris Sud 11, 1 Avenue Fresnel, 91767 Palaiseau, France

M. D. Stiles

*Center for Nanoscale Science and Technology, National Institute of
Standards and Technology, Gaithersburg, Maryland 20899-6202, USA*

Spin-orbit coupling in ferromagnets gives rise to the anomalous Hall effect and the anisotropic magnetoresistance, both of which can be used to create spin-transfer torques in a similar manner as the spin Hall effect. In this paper we show how these effects can be used to reliably switch perpendicularly magnetized layers and to move domain walls. A drift-diffusion treatment of the anomalous Hall effect and the anisotropic magnetoresistance describes the spin currents that flow in directions perpendicular to the electric field. In systems with two ferromagnetic layers separated by a spacer layer, an in-plane electric field cause spin currents to be injected from one layer into the other, creating spin transfer torques. Unlike the related spin Hall effect in non-magnetic materials, the anomalous Hall effect and the anisotropic magnetoresistance allow control of the orientation of the injected spins, and hence torques, by changing the direction of the magnetization in the injecting layer. The torques on one layer show a rich angular dependence as a function of the orientation of the magnetization in the other layer. The control of the torques afforded by changing the orientation of the magnetization in a fixed layer makes it possible to reliably switch a perpendicularly magnetized free layer. Our calculated critical current densities for a representative CoFe/Cu/FePt structure show that the switching can be efficient for appropriate material choices. Similarly, control of the magnetization direction can drive domain wall motion, as shown for NiFe/Cu/NiFe structures.

I. INTRODUCTION

The use of spin-orbit coupling to generate spin-transfer torques¹⁻⁵ raises the possibility of new types of devices and more efficient versions of existing devices. In general, the spin-orbit coupling in these studies has been provided by a non-magnetic heavy metal layer such as Pt. Here, we show that replacing this non-magnetic layer by a ferromagnetic layer and a thin spacer layer offers potential advantages in device design. In existing approaches, spin-orbit torques^{6,7} typically derive from the spin Hall effect⁸⁻¹⁰ in the bulk of non-magnetic layers or from spin-orbit torques localized at the interface between such a layer and a ferromagnetic layer.¹¹⁻¹⁹ The resulting torques may lead to more efficient switching of memory elements²⁰⁻²⁴ or domain wall motion.²⁵⁻³¹ Considerable experimental³²⁻³⁷ and theoretical³⁸⁻⁴² work has been devoted to characterizing these torques so as to understand the details of their origin. However, device design possibilities based on heavy metal layers are somewhat limited by the fact that the form of the torques is determined by the geometry of the device, that is, the direction of the current flow and the interface normal. We show that replacing the non-magnetic heavy metal by a ferromagnetic layer and a thin spacer layer gives greater control over the form of the torque because it is controlled by

the direction of the magnetization, which can be varied, rather than the geometry.

Historically, the earliest spintronic effects, discovered before the electron was known to have a spin, were the anisotropic magnetoresistance,^{43,44} and the anomalous Hall effect.⁴⁵⁻⁴⁹ Both of these effects are caused by spin-orbit coupling, but because of the strong coupling between spin currents and charge currents in ferromagnets, these are typically discussed in terms of the resulting charge currents and voltages. Very recently, several groups⁵⁰⁻⁵⁴ measured what they described as the inverse spin Hall effect in permalloy, a nickel-iron alloy. This result raises the point that a spin current will always accompany the charge current caused by the anomalous Hall effect¹⁰ and the spin current will vary with the angle between the magnetization and the charge current as in the anisotropic magnetoresistance. We show that both the anomalous Hall effect and anisotropic magnetoresistance can be exploited to generate spin currents and spin transfer torques in much the same way as the spin Hall effect.

The spin Hall effect⁸⁻¹⁰ occurs in metals, particularly heavy metals with strong spin-orbit coupling. When an electric field is applied in a particular direction, a spin current flows in all directions perpendicular to the field with spins oriented perpendicularly to their flow. That

is, for an electric field in the $\hat{\mathbf{E}}$ direction, there is a spin current in every direction \mathbf{e} perpendicular to the electric field $\hat{\mathbf{e}} \cdot \hat{\mathbf{E}} = 0$ with spins pointing in the $\hat{\mathbf{e}} \times \hat{\mathbf{E}}$ direction. This spin current can be written in the form $Q_{ij} = (-\hbar/2e)\sigma_{\text{SH}}\epsilon_{ijk}E_k$, where the second index of the tensor spin current \mathbf{Q} refers to the real space direction of flow and the first index refers to the orientation of the spin that is flowing. \mathbf{E} is the electric field, σ_{SH} is the spin Hall conductivity, and ϵ_{ijk} is the Levi-Civita symbol. Repeated indices (here k) are summed over (here summing over $k = x, y, z$). The spin current arises through either intrinsic mechanisms,^{55,56} that is through the spin-orbit coupling in the band structure, or extrinsic mechanisms^{57,58} through the spin-orbit coupling in the impurity scattering.

The same spin-orbit effects occur in ferromagnets but are complicated by the exchange potential that gives rise to spin split band structures and spin-dependent conductivities. One complication is that in a ferromagnet any spin that is transverse to the magnetization precesses rapidly, so any transverse spin accumulation or spin current dephases quickly due to this precession. Thus, it becomes a very good approximation to treat the spins in a ferromagnet as parallel or antiparallel to the magnetization. Then, the tensor spin current in a ferromagnet has spins pointing in the direction of the magnetization \mathbf{m} flowing in the \mathbf{j}_s direction, or $\mathbf{Q} \sim \mathbf{m} \otimes \mathbf{j}_s$. This feature plays a crucial role in the results below. It allows control of the direction of the spins injected into other layers due to spin-orbit effects simply by changing \mathbf{m} . Such control does not exist with the spin Hall effect where the direction the spins point when injected into another layer is $\mathbf{n} \times \mathbf{E}$, where \mathbf{n} is the interface normal direction.

A second complication is that majority and minority electrons see very different potentials so the spin-orbit scattering that gives rise to pure spin currents in non-magnets gives rise to a charge current as well as a spin current. This charge current is the current measured in the anomalous Hall effect, whose direction is given by $\mathbf{m} \times \mathbf{E}$. Therefore, the spin current excited by the anomalous Hall effect has spins pointing the \mathbf{m} direction flowing in the $\mathbf{m} \times \mathbf{E}$ direction, that is

$$\begin{aligned} \mathbf{Q} &= \frac{-\hbar}{2e}\zeta\sigma_{\text{AH}}\mathbf{m} \otimes \mathbf{m} \times \mathbf{E} \\ Q_{ij} &= \frac{-\hbar}{2e}\zeta\sigma_{\text{AH}}m_i\epsilon_{jkl}m_kE_l. \end{aligned} \quad (1)$$

The anomalous Hall conductivity, σ_{AH} , describes the charge current due to the anomalous Hall effect, the associated polarization ζ expresses the fact that this charge current is spin polarized.

The anisotropic magnetoresistance^{43,44} is an additional consequence of spin-orbit coupling in ferromagnets. In this case, the conductivity of a ferromagnet is different if the magnetization is along the electric field direction or perpendicular to it. While not typically considered, the polarization of the conductivity will change in these two

cases. Another consequence of the anisotropy in the conductivity occurs when the magnetization is at any angle other than collinear with or perpendicular to the electric field. For these other orientations of the magnetization, the charge current has an additional contribution, which flows in the direction of the magnetization. This current is frequently described as the planar Hall effect because for a thin film ferromagnet, an electric field gives rise to a Hall current (perpendicular to the electric field) when the magnetization is rotated in the plane of the film. The charge current direction due to the planar Hall effect is given by $\mathbf{m}(\mathbf{m} \cdot \mathbf{E})$ and again, the spins flowing with that current point the \mathbf{m} direction. Then, the anisotropic magnetoresistance gives rise to a spin current

$$\begin{aligned} \mathbf{Q} &= \frac{-\hbar}{2e}\eta\sigma_{\text{AMR}}\mathbf{m} \otimes \mathbf{m}(\mathbf{m} \cdot \mathbf{E}) \\ Q_{ij} &= \frac{-\hbar}{2e}\eta\sigma_{\text{AMR}}m_im_jm_kE_k. \end{aligned} \quad (2)$$

The conductivity, σ_{AMR} , describes the difference in the charge conductivity comparing cases with the magnetic field parallel and perpendicular to the electric field. The associated polarization η expresses the fact that this change in the charge current is spin polarized. The spins both flow and point along the magnetization.

The spin currents associated with the anomalous Hall effect and the anisotropic magnetoresistance can replace those associated with the spin Hall effect as generators of torques with advantage of being able to control the orientation of the spins. Applying an electric field in the plane of a ferromagnetic layer generates charge and spin currents flowing perpendicular to it and into adjacent layers. Thus in a FM/NM/FM film, where FM and NM refer to ferromagnetic and non-magnetic layers respectively, an in-plane electric field generates spin currents flowing perpendicularly to the layers. These spin currents exert torques on the magnetizations in both layers. The advantage of this approach is the orientation of the flowing spins can be controlled by varying the directions of the magnetizations. The goal of this paper is to evaluate these spin transfer torques and show how they may be advantageous for some device applications. We develop the drift-diffusion equations in Sec. II and apply them to the case in which an electric current flows in the plane of a FM/NM/FM film. Details of the derivation are given in the Appendices. In Sec. III, we illustrate the angular dependence of the torque as both magnetizations are varied and then show how these torques can lead to effective magnetization switching and domain wall motion. We summarize our results in Sec. IV.

II. DERIVATION

In this section we present the drift diffusion equations in ferromagnets, accounting for the spin-orbit derived contributions to the transport. Since spin com-

ponents transverse to the magnetization rapidly precess and dephase, they can be neglected. Then, the charge and spin currents are combinations of the majority and minority currents carried by spin- s ($s = \uparrow, \downarrow$) electrons. In the presence of the Anomalous Hall (AH) effect and the anisotropic magnetoresistance (AMR) effect, the spin current densities are given by

$$\mathbf{j}^\uparrow = \frac{(1+\beta)}{2} \frac{\sigma}{e} \nabla \mu^\uparrow + \frac{(1+\zeta)}{2} \frac{\sigma_{\text{AH}}}{e} \mathbf{m} \times \nabla \mu^\uparrow + \frac{(1+\eta)}{2} \frac{\sigma_{\text{AMR}}}{e} \mathbf{m} (\mathbf{m} \cdot \nabla \mu^\uparrow), \quad (3)$$

$$\mathbf{j}^\downarrow = \frac{(1-\beta)}{2} \frac{\sigma}{e} \nabla \mu^\downarrow + \frac{(1-\zeta)}{2} \frac{\sigma_{\text{AH}}}{e} \mathbf{m} \times \nabla \mu^\downarrow + \frac{(1-\eta)}{2} \frac{\sigma_{\text{AMR}}}{e} \mathbf{m} (\mathbf{m} \cdot \nabla \mu^\downarrow), \quad (4)$$

where the (total) electric current density is $\mathbf{j} = \mathbf{j}^\uparrow + \mathbf{j}^\downarrow$. The longitudinal conductivity and conductivities due to the anomalous Hall effect and the anisotropic magnetoresistance effect are denoted as σ , σ_{AH} , and σ_{AMR} , respectively, and their spin polarizations are denoted as β , ζ , and η respectively. The spin-dependent electro-chemical potentials are denoted as μ^s . We define electro-chemical potential $\bar{\mu}$ and spin accumulation $\delta\mu$ as

$$\bar{\mu} = \frac{\mu^\uparrow + \mu^\downarrow}{2}, \quad \delta\mu = \frac{\mu^\uparrow - \mu^\downarrow}{2}. \quad (5)$$

We emphasize that the "(longitudinal) spin accumulation" used in Refs. 59–61, which will be used below, is defined as $\mu^\uparrow - \mu^\downarrow$, which is twice the magnitude of $\delta\mu$. In terms of $\bar{\mu}$ and $\delta\mu$, we find that

$$\begin{aligned} \mathbf{j}^\uparrow + \mathbf{j}^\downarrow &= \frac{\sigma}{e} \nabla \bar{\mu} + \beta \frac{\sigma}{e} \nabla \delta\mu \\ &+ \frac{\sigma_{\text{AH}}}{e} \mathbf{m} \times \nabla \bar{\mu} + \zeta \frac{\sigma_{\text{AH}}}{e} \mathbf{m} \times \nabla \delta\mu \\ &+ \frac{\sigma_{\text{AMR}}}{e} \mathbf{m} (\mathbf{m} \cdot \nabla \bar{\mu}) + \eta \frac{\sigma_{\text{AMR}}}{e} \mathbf{m} (\mathbf{m} \cdot \nabla \delta\mu), \end{aligned} \quad (6)$$

$$\begin{aligned} \mathbf{j}^\uparrow - \mathbf{j}^\downarrow &= \frac{\sigma}{e} \nabla \delta\mu + \beta \frac{\sigma}{e} \nabla \bar{\mu} \\ &+ \frac{\sigma_{\text{AH}}}{e} \mathbf{m} \times \nabla \delta\mu + \zeta \frac{\sigma_{\text{AH}}}{e} \mathbf{m} \times \nabla \bar{\mu} \\ &+ \frac{\sigma_{\text{AMR}}}{e} \mathbf{m} (\mathbf{m} \cdot \nabla \delta\mu) + \eta \frac{\sigma_{\text{AMR}}}{e} \mathbf{m} (\mathbf{m} \cdot \nabla \bar{\mu}). \end{aligned} \quad (7)$$

In terms of these current densities, the tensor spin current density is $\mathbf{Q} = -\frac{\hbar}{2e} \mathbf{m} \otimes (\mathbf{j}^\uparrow - \mathbf{j}^\downarrow)$.

It is tempting to imagine that all three polarizations, β , ζ , and η are the same, but there is no reason that they should be. The polarization of the longitudinal conductivity, β is determined by the spin-dependent densities of states and particularly the spin-dependent scattering rates. It is typically between -1 and 1, with negative values for the rare cases in which the minority conductivity is higher than the majority. Values approach ± 1 for half metals. Values greater than 1 or less than -1 would imply that one spin type move backwards. We are not aware

of any such case.

The polarizations, *zeta*, that of polarization of the anomalous Hall effect and η , that of the anomalous Hall effect are not simply related to β . For example, we can construct several contradictory arguments for the value of *zeta*. If we imagine that the anomalous Hall effect were simply a deflection of all carriers in one direction and that these carriers then underwent the same spin-dependent scattering as the longitudinal current, we would guess that $\zeta \approx \frac{(1+\beta)\sigma_{\text{AH}} - (1-\beta)\sigma_{\text{AH}}}{(1+\beta)\sigma_{\text{AH}} + (1-\beta)\sigma_{\text{AH}}} = \beta$. If on the other hand, we imagine that the anomalous Hall effect originates from the spin Hall effect in which different spins are deflected in opposite directions and then each spin is subject to the same spin-dependent scattering, we might imagine that the majority and minority electrons flow in the opposite directions but are affected by the same spin dependent scattering as the conductivity. The reversed flow for the minority electrons essentially inverts the polarization $\zeta \approx \frac{(1+\beta)\sigma_{\text{AH}} + (1-\beta)\sigma_{\text{AH}}}{(1+\beta)\sigma_{\text{AH}} - (1-\beta)\sigma_{\text{AH}}} = 1/\beta$. In fact, first principles calculations⁶² of the spin polarization of the anomalous Hall effect give results that vary widely and do not seem to agree with any simple model. Some of this variability can be understood from first principles calculations⁵⁶ of the spin Hall effect, which show that the spin Hall conductivity depends sensitively on the Fermi level. The spin split-band structure of ferromagnets can be viewed in a simple approximation as just a shift in energies of the bands for one spin relative to the other, or equivalently the two spins see different Fermi energies. In this case, the minority and majority spins that are deflected in different directions are deflected by different potentials and will be deflected in different amounts. Therefore, part of the polarization ζ of the anomalous Hall current comes from the energy dependence of the "underlying spin Hall effect." Similarly, η , the spin polarization of the anomalous Hall effect, is determined by the change in the spin-dependent scattering and as such gives no expectation to its value.

We are interested in the geometry, illustrated in Fig. 1(b), in which two ferromagnetic films are separated from each other by a thin non-magnetic layer that allows the magnetizations of the two layers to be oriented independently of each other. We assume that the interface normals lie in the z -direction and the electric field is applied in the x -direction. We ignore charge and spin currents that flow in the y -direction because they do not couple to anything. In general, an electric field in the x -direction would give rise to charge current flow in the z -direction, but the thin film geometry treated here prevents that. Except for the applied electric potential $eE_x x$, only the z -components of $\nabla \bar{\mu}$ and $\nabla \delta\mu$ are non-zero, i.e., $\nabla(\bar{\mu}/e) = E_x \mathbf{e}_x + (\partial_z \bar{\mu}/e) \mathbf{e}_z$ and $\nabla(\delta\mu/e) = (\partial_z \delta\mu/e) \mathbf{e}_z$. The electric field adjusts itself so that no electric current flows in the z -direction.

In a particular ferromagnetic layer, we can solve

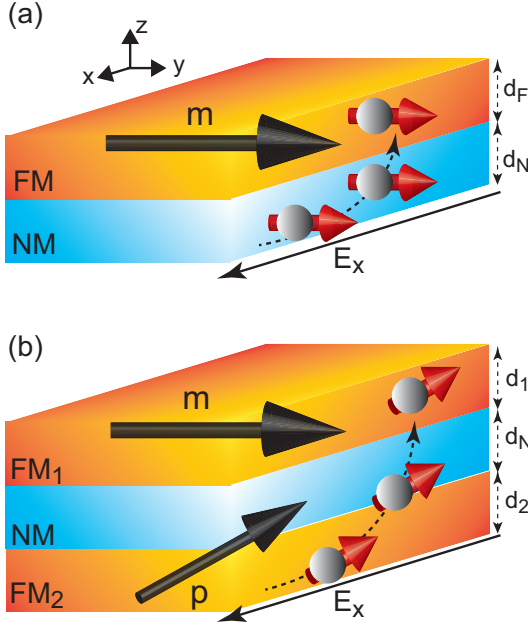


FIG. 1: (color online) (a) Schematic geometry for spin Hall effect induced spin transfer torques. In this geometry, the damping-like torque is with respect to the y -axis, i.e. $\mathbf{m} \times (\hat{\mathbf{y}} \times \mathbf{m})$ (with a smaller field-like torque). (b) Schematic geometry for anomalous Hall effect induced spin transfer torques. In this case, the damping-like torque is with respect to the fixed layer magnetization direction \mathbf{p} , i.e. $\mathbf{m} \times (\mathbf{p} \times \mathbf{m})$ (with a smaller field-like torque).

Eqs. (6) and (7) together with the diffusion equation⁶³

$$\frac{\partial^2}{\partial z^2}(\mu^\uparrow - \mu^\downarrow) = \frac{\mu^\uparrow - \mu^\downarrow}{\ell_{\text{sf}}^2}, \quad (8)$$

where ℓ_{sf} is the spin diffusion length. In Appendix A, we give the details the derivation of these solutions. Here we highlight some of the key steps. Forcing the charge current in the z -direction to be zero dictates that the spin current in the z -direction have the form

$$j_z^\uparrow - j_z^\downarrow = \tilde{\sigma}_E E_x + \frac{\tilde{\sigma}_{\delta\mu}}{2e\ell_{\text{sf}}} \left(A e^{z/\ell_{\text{sf}}} - B e^{-z/\ell_{\text{sf}}} \right), \quad (9)$$

where the constants A and B are to be determined in Appendix A. The spin current is given in terms of two effective conductivities $\tilde{\sigma}_E$ and $\tilde{\sigma}_{\delta\mu}$. The former essentially gives the spin current that would result in a bulk material in response to a field in the x -direction in which the transverse charge current were constrained to be zero. The latter gives the spin current in response to a spin accumulation, including the corrections due to the charge current itself being zero. The effective conductivities are

$$\begin{aligned} \tilde{\sigma}_E &= \frac{(\beta\sigma + \eta\sigma_{\text{AMR}}m_z^2)(\sigma_{\text{AH}}m_y - \sigma_{\text{AMR}}m_zm_x)}{\sigma + \sigma_{\text{AMR}}m_z^2} \\ &\quad - (\zeta\sigma_{\text{AH}}m_y - \eta\sigma_{\text{AMR}}m_zm_x), \end{aligned} \quad (10)$$

and

$$\begin{aligned} \tilde{\sigma}_{\delta\mu} &= \sigma + \sigma_{\text{AMR}}m_z^2 \\ &\quad - (\beta\sigma + \eta\sigma_{\text{AMR}}m_z^2) \left(\frac{\beta\sigma + \eta\sigma_{\text{AMR}}m_z^2}{\sigma + \sigma_{\text{AMR}}m_z^2} \right). \end{aligned} \quad (11)$$

While the effective conductivities appear complicated, $\tilde{\sigma}_E$ simplifies considerably in certain limits and gives simple illustrations of the main results of this paper. If the anisotropic magnetoresistance can be neglected, $\tilde{\sigma}_E \rightarrow (\beta - \zeta)m_y\sigma_{\text{AH}}$. Thus, there is a spin current whenever the magnetization has a component along the y -direction, $Q_{iz} \sim m_i m_y$. This means that by tilting the magnetization out-of-plane, it is possible to get an out-of-plane component the spins flowing into the other layer, something not achievable with the spin Hall effect in non-magnetic materials. This feature is illustrated in Fig 1(b). The factor of $(\beta - \zeta)$ arises from two contributions, the term proportional to ζ is directly from the polarized current accompanying the anomalous Hall current. The term proportional to β comes from the polarization of the “counter-flow” current that cancels the anomalous Hall current.

When the anomalous Hall effect can be neglected, $\tilde{\sigma}_E \rightarrow (\eta - \beta)m_x m_z \sigma_{\text{AMR}} \frac{\sigma}{\sigma + \sigma_{\text{AMR}}m_z^2}$. This expression is more complicated than that for the anomalous Hall effect above because the anisotropic magnetoresistance affects the conductivity in the z -direction as captured by the last factor in this expression. As with the previous case, an out-of plane component of the magnetization gives an out-of-plane component to the spin current, $Q_{iz} \sim m_i m_x m_z$. As with the previous case, the factor of $(\eta - \beta)$ appears from the polarized current due to the planar Hall effect and the counter-flow current that cancels the charge current of the planar Hall effect.

Computing the torques on both layers requires finding the spin accumulation and spin current throughout the structure. The spin current at the F_1/N interface is given in terms of the spin accumulation at the F_1/N interface and interface conductances.^{59–61} The spin accumulation is found by applying appropriate boundary conditions to $\bar{\mu}$ and $\delta\mu$ as described in Appendix A. For a magnetic layer with interface (1) at $z = 0$ and interface (2) at $z = d$, we have

$$\begin{aligned} \tilde{\sigma}_{\delta\mu}(\mu^\uparrow - \mu^\downarrow) &= \frac{-2e\ell_{\text{sf}}}{\sinh(d/\ell_{\text{sf}})} \\ &\quad \times \left[\left(j_{sz}^{(1)} - \tilde{\sigma}_E E_x \right) \cosh\left(\frac{z-d}{\ell_{\text{sf}}}\right) \right. \\ &\quad \left. - \left(j_{sz}^{(2)} - \tilde{\sigma}_E E_x \right) \cosh\left(\frac{z}{\ell_{\text{sf}}}\right) \right] \end{aligned} \quad (12)$$

where $\mathbf{j}_s^{(i)}$ is $\mathbf{j}^\uparrow - \mathbf{j}^\downarrow$ at the interface of the normal metal

with ferromagnet i . The spin current is then

$$\mathbf{Q}_s^{F_1 \rightarrow N} = \frac{1}{4\pi} \left[\frac{(1 - \gamma^2)g}{2} \mathbf{m} \cdot (\boldsymbol{\mu}_{F_1} - \boldsymbol{\mu}_N) \mathbf{m} - g_r \mathbf{m} \times (\boldsymbol{\mu}_N \times \mathbf{m}) - g_i \boldsymbol{\mu}_N \times \mathbf{m} \right]. \quad (13)$$

Here $g = g^{\uparrow\uparrow} + g^{\downarrow\downarrow}$ and $\gamma = (g^{\uparrow\uparrow} - g^{\downarrow\downarrow})/g$ are the dimensionless interface conductance and its spin polarization, respectively, which relates to the interface resistance r via $r = [(1/r^{\uparrow\uparrow}) + (1/r^{\downarrow\downarrow})]^{-1} = (\hbar/e^2)S/g$ with $\hbar/e^2 = 25.9 \text{ k}\Omega$. The cross section area is denoted as S . The real and imaginary parts of the mixing conductance are denoted as g_r and g_i , respectively. Note that the charge chemical potential does not appear because the fact that the charge current across the interface is zero allows us to relate the chemical potential difference to the longitudinal spin chemical potential difference and eliminate the former from the equation for the spin current.

The solutions of the spin accumulations in each ferromagnetic layer and the boundary conditions allow us to write the spin current in each ferromagnetic layer in terms of the just the spin accumulation in the non-magnetic layer

$$\begin{aligned} \mathbf{Q}_s^{F_1 \rightarrow N} = & \frac{\hbar g^*}{2e g'_{sd}} \tanh\left(\frac{d_1}{2\ell_{sf}}\right) \tilde{\sigma}_E E_x S \mathbf{m} \\ & - \frac{1}{4\pi} [g^* (\mathbf{m} \cdot \boldsymbol{\mu}_N) \mathbf{m} \\ & + g_r \mathbf{m} \times (\boldsymbol{\mu}_N \times \mathbf{m}) + g_i \boldsymbol{\mu}_N \times \mathbf{m}], \end{aligned} \quad (14)$$

where g^* is defined as

$$\frac{1}{g^*} = \frac{2}{(1 - \gamma^2)g} + \frac{1}{g'_{sd} \tanh(d_1/\ell_{sf})}, \quad (15)$$

and

$$\frac{g'_{sd}}{S} = \frac{\hbar \tilde{\sigma}_\delta \mu}{2e^2 \ell_{sf}}. \quad (16)$$

Similarly, the spin current at the F_2/N interface is given by

$$\begin{aligned} \mathbf{Q}_s^{F_2 \rightarrow N} = & -\frac{\hbar g^*}{2e g'_{sd}} \tanh\left(\frac{d_2}{2\ell_{sf}}\right) \tilde{\sigma}_E E_x S \mathbf{p} \\ & - \frac{1}{4\pi} [g^* (\mathbf{p} \cdot \boldsymbol{\mu}_N) \mathbf{p} \\ & + g_r \mathbf{p} \times (\boldsymbol{\mu}_N \times \mathbf{p}) + g_i \boldsymbol{\mu}_N \times \mathbf{p}]. \end{aligned} \quad (17)$$

In the structure in Fig 1, we separate the two ferromagnetic layers by a thin non-magnetic layer. We assume that this layer effectively breaks the exchange coupling between the two ferromagnetic layers. We also assume that it is still thinner than its mean free path and spin diffusion length, so that spin current injected at one interface transmits unchanged to the other interface. These assumptions imply that the spin current and spin accu-

mulation in the spacer layer can be treated as constant. This condition means that $\mathbf{Q}_s^{F_1 \rightarrow N} + \mathbf{Q}_s^{F_2 \rightarrow N} = \mathbf{0}$, from which $\boldsymbol{\mu}_N$ can be determined. Then, the spin torque acting on \mathbf{m} is obtained from

$$\mathbf{T} = \left(\frac{d\mathbf{m}}{dt} \right)_{st} = \frac{\gamma_0}{\mu_0 M_s V} \mathbf{m} \times (\mathbf{Q}_s^{F_1 \rightarrow N} \times \mathbf{m}), \quad (18)$$

where μ_0 is the magnetic constant and, γ_0 , M_s , and V are the gyromagnetic ratio, saturation magnetization, and volume of F_1 , respectively.

Further progress requires taking these solutions for both ferromagnetic layers and solving for the spin accumulation in the non-magnetic layer. In general, the resulting torque can be written in the form

$$\begin{aligned} \mathbf{T} = & \frac{\gamma_0 \hbar E_x}{2e \mu_0 M_s d_1} \\ & [\sigma_{\text{eff}}^d(\mathbf{m}, \mathbf{p}) \mathbf{m} \times (\mathbf{p} \times \mathbf{m}) + \sigma_{\text{eff}}^f(\mathbf{m}, \mathbf{p}) \mathbf{p} \times \mathbf{m}] \end{aligned} \quad (19)$$

The superscripts on the effective conductivities refer to the damping-like, d , and field-like, f , components of the torque. However, a key point of this paper is that these damping-like and field-like torques are defined with respect to the orientation of the magnetization in the other layer, here \mathbf{p} , and not as for the spin Hall effect, the direction $\hat{\mathbf{E}} \times \hat{\mathbf{n}}$, where $\hat{\mathbf{n}}$ is the interface normal. See Fig. 1 for the comparison. The effective conductivities depend strongly on the directions of the magnetizations, \mathbf{m} and \mathbf{p} . In particular, they inherit the strong orientational dependence from $\tilde{\sigma}_E$. When the imaginary part of the mixing conductance can be neglected, the field-like torque vanishes. The spin torque acting on \mathbf{p} is obtained in a similar way. In Appendix B, we show how to compute the torques numerically for the general case and show some analytic forms for some special cases. In the next section, we present numerical results and investigate the consequences of these torques on switching and domain wall motion.

The derivation in this section is done using the drift-diffusion approach, as is typically used in the analysis of experiments using the spin Hall effect to generate spin transfer torques. This approximation does not capture the in-plane giant magnetoresistance effect because in the absence of spin orbit effects, there is no net spin current flowing from layer to layer. The simplest calculation to capture the current-in-plane giant magnetoresistance is based on the Boltzmann equation.⁶⁴ When applied to the spin Hall effect and resulting torques, this approach³⁸ yields quantitative but not qualitative differences in comparison with the drift diffusion approach. We expect the same to be true for the present calculations. It is also the case that the in-plane giant magnetoresistance, in the absence of spin-orbit coupling, does not lead to a spin transfer torque even though spin flow from each layer to the other.

	NiFe	CoFeB	FePt	units
ρ	122 ^a	300 ^b	390 ^c	Ωnm
β	0.7 ^a	0.56 ^b	0.40 ^d	
r	0.5 ^a	0.5 ^b	0.5	$\text{k}\Omega\text{nm}^2$
γ	0.7 ^a	0.83 ^b	0.83	
g_r/S	10.0 ^e	10.0	10.0	nm^{-2}
g_i/S	1.0	0.0	0.0	nm^{-2}
ℓ_{sf}	5.5 ^a	4.5 ^f	5.0 ^d	nm
$\sigma_{\text{AH}}/\sigma$	0.001 ^g	0.0	0.015 ^c	
$\sigma_{\text{AMR}}/\sigma$	0.06 ^h	0.0	0.0147 ⁱ	
ζ	5	0	1.5	
η	0.9	0	-0.1	
M_s	0.86 ^j	0.456 ^k		MA/m
H_K	0.0	0.569 ^k		MA/m
γ_0	0.23206	0.23206		$\text{Mm}/(\text{A s})$
α	0.01 ^j	0.01		

TABLE I: Default material parameters. Parameters are chosen to approximate $\text{Ni}_{80}\text{Fe}_{20}$ (Permalloy), CoFeB and FePt, but some values are not well known. In particular, η and ζ are unknown to our knowledge and so we have chosen representative values. Values for parameters are taken from (a) Ref. 65, (b) Ref. 66 (c) Ref. 67, (d) Ref. 68, (e) Ref. 69 (f) Ref. 70, (g) Ref. 71, (h) Ref. 72, (i) Ref. 73, (j) Ref. 74, (k) Ref. 75, (l) Ref. 76 where indicated and estimated where not indicated.

III. RESULTS

A. Angular dependence of torques

While the full solution of the torque for a general model is quite complicated, it can be qualitatively understood much more simply. Using the parameters in Table I, we compute the torque for a variety of magnetization directions for two 5 nm thick NiFe layers and plot them in Fig. 2. For simplicity, we consider two cases, $\sigma_{\text{AMR}} = 0$ and $\sigma_{\text{AH}} = 0$, so we can show the effect of each separately. In the limit that both are much less than σ , the two contributions should add.

Consider first the case in which there is only the anomalous Hall effect. We have assumed that the imaginary part of the mixing conductance is much less than the real part, so any field-like torque that is present is also much smaller than the damping-like contribution. The discussion in Sec. I that $\tilde{\sigma}_E (\beta - \zeta)p_y\sigma_{\text{AH}}$ for the spin current due to the fixed layer with its magnetization in the \mathbf{p} direction, gives guidance for the approximate angular dependence of the torque. Since the spins in the spin current point in the \mathbf{p} direction, the damping-like torque varies like $p_y\mathbf{m} \times (\mathbf{p} \times \mathbf{m})$. When the magnetization is along the y -axis, the torque has the same angular dependence as the spin Hall effect as seen in the heavy (red) curves of Fig. 2(e-j). That is, a damping-like torque with respect to the y -axis. In this case, the out-of-plane

torque, T_z , (heavy red curve in Fig. 2(g)) is essentially zero when the magnetization is rotated in plane.

As the fixed layer magnetization is rotated out of plane (light (green) and dashed (blue) curves in Fig. 2(e-j)), the torque remains damping-like, $p_y\mathbf{m} \times (\mathbf{p} \times \mathbf{m})$, but it develops an out-of-plane component, T_z , even when the magnetization is rotated in plane, (light (green) and dashed (blue) curves in Fig. 2(g)). This breaks the symmetry between $\mathbf{m} = \pm\hat{\mathbf{z}}$, making it possible to reliably switch the magnetization, as discussed in the next section. However, as the polarizer magnetization is rotated toward the pole, the total size of the torque goes to zero because p_y goes to zero when $p_z \rightarrow \pm 1$.

When the anomalous Hall effect is absent and the anisotropic magnetoresistance is present (Fig. 2(k-p)), the angular dependence is slightly more complicated. Recall from Sec. I that $\tilde{\sigma}_E \rightarrow (\eta - \beta)p_x p_z \sigma_{\text{AMR}} \frac{\sigma}{\sigma + \sigma_{\text{AMR}} p_z^2}$ when the anomalous Hall effect is absent. If $\sigma_{\text{AMR}}/\sigma \ll 1$, the last factor can be neglected. In that case, the damping-like torque varies like $p_x p_z \mathbf{m} \times (\mathbf{p} \times \mathbf{m})$. The spin current flows along the magnetization direction, so unless $p_z \neq 0$ there is no spin current flow into the free layer. Thus, the torque is zero when the fixed layer magnetization is in-plane (heavy (red) curves in Fig. 2(k-p)). Otherwise, it has roughly a damping-like form with respect to the fixed layer magnetization. For the values of parameters we have assumed, there are deviations from the simple $\mathbf{m} \times (\mathbf{p} \times \mathbf{m})$ behavior expected when the spin-orbit effects are weak.

B. Magnetic Switching

One advantage of spin-orbit effects in ferromagnets, as compared to the spin Hall effect, is that the control over the direction of the incident spin current allows for the excitation of magnetization dynamics that cannot be excited by the spin Hall effect. An example of such dynamics is a switching of a perpendicularly magnetized free layer in the absence of an external field. In this section, we analytically compute the critical current for switching a perpendicular magnetization in F_1 due to the anomalous Hall effect and anisotropic magnetoresistance effect in F_2 . We verify the behavior by direct numerical simulation of the Landau-Lifshitz-Gilbert (LLG) equation.

For illustrative purposes, we simplify the generally complex dependence on relative angle of the magnetizations seen in Eq. (B18) by treating a special case. We assume that F_1 has neither the anomalous Hall effect nor the anisotropic magnetoresistance, i.e., $\sigma_{\text{AH}(F_1)} = \sigma_{\text{AMR}(F_1)} = 0$, whereas F_2 has both. The magnetization of F_1 , \mathbf{m} , can move freely, whereas that of F_2 , \mathbf{p} , points to an arbitrary fixed direction. The values of the parameters are taken from CoFeB free (F_1) layer and FePt pinned (F_2) layer, and summarized in Table I.

The LLG equation for the magnetization in F_1 , with

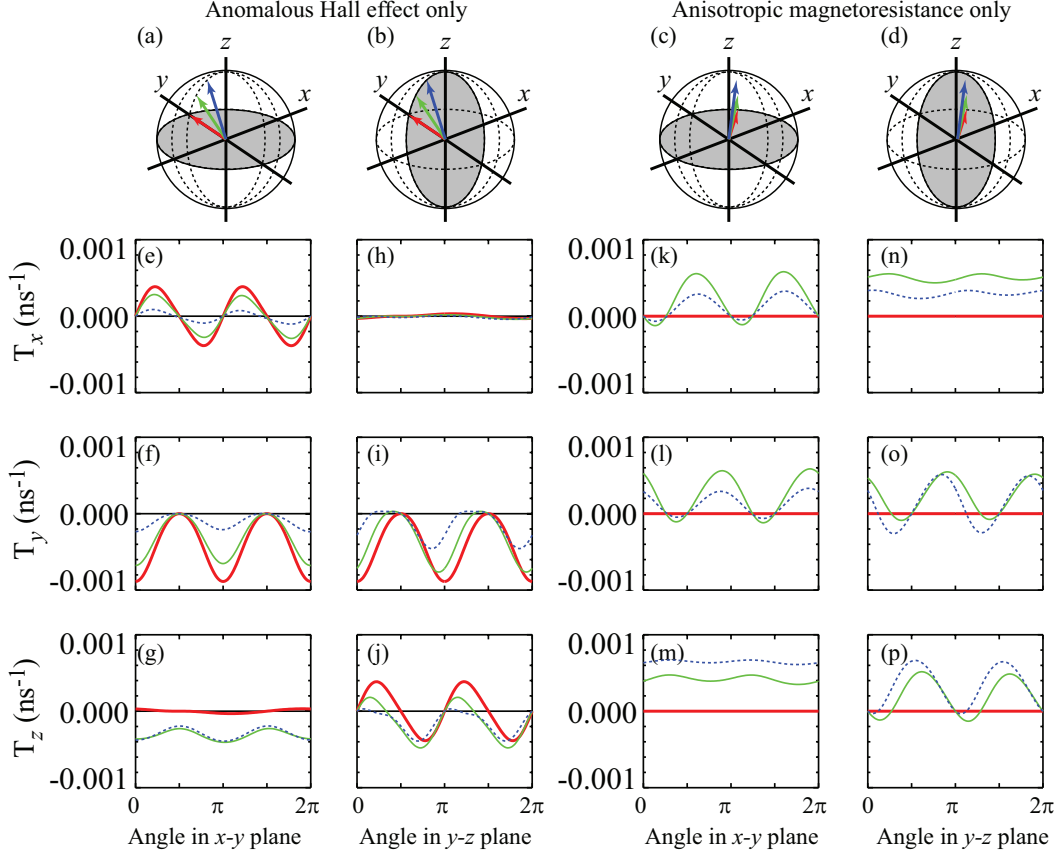


FIG. 2: (color online) Angular dependence of spin transfer torques. Panels (a) through (d) show the directions of the magnetizations in each column. The gray projected circles indicate the plane of rotation of the free layer magnetization, \mathbf{m} . For panels (a) and (c) the plane of rotation is the $x - y$ plane, starting at $\hat{\mathbf{x}}$ and for panels (b) and (d) it is the $y - z$ plane starting at $\hat{\mathbf{z}}$. The arrows in panels (a-d) indicate the three directions of the fixed layer magnetization, \mathbf{p} for the panels in each column (online, the colors correspond to the colors of the curves in the panels below). These are at $\theta = 90^\circ$, 60° , and 30° for all four panels and $\phi = 90^\circ$ for (a) and (b) and $\phi = 45^\circ$ for (c) and (d). Panels (e-j) give the torques for the anomalous Hall effect with the anisotropic magnetoresistance set to zero and panels (k-p) the other way around. In each of the panels (e-p) the heavy (red) lines give the torque for $\theta = 90^\circ$, light (green) lines for $\theta = 60^\circ$ and dashed (blue) for $\theta = 30^\circ$. Rows (e,h,k,n), (f,i,l,o), and (g,j,m,p) give the x , y , and z components of the torque respectively. For all calculations, the current density is 10^{11} A/m 2 .

the spin torque, Eq. (19), is

$$\begin{aligned} \frac{d\mathbf{m}}{dt} = & -\gamma_0 \mathbf{m} \times \mathbf{H} + \alpha \mathbf{m} \times \frac{d\mathbf{m}}{dt} \\ & + \frac{\gamma_0 \hbar}{2e\mu_0 M_s d_1} E_x \sigma_{\text{eff}}^d \mathbf{m} \times (\mathbf{p} \times \mathbf{m}), \end{aligned} \quad (20)$$

where α is the Gilbert damping constant, and σ_{eff}^d is given by (see also Appendix B)

$$\sigma_{\text{eff}}^d = \frac{\tanh[d_2/(2\ell_{\text{sf}}^2)] g_{\text{r}(\text{F}_1)} g_{\text{F}_2}^*(\mathbf{p}) \tilde{\sigma}_{E(\text{F}_2)}(\mathbf{p})}{g'_{\text{sd}(\text{F}_2)}(\mathbf{p}) (g_{\text{r}(\text{F}_1)} + g_{\text{F}_2}^*(\mathbf{p})) [1 - \lambda_1 \lambda_2(\mathbf{p}) (\mathbf{m} \cdot \mathbf{p})^2]}. \quad (21)$$

We introduce the parameter λ_k ($k = 1, 2$), which characterizes the dependence of the spin torque strength on

the relative angle of the magnetizations,

$$\lambda_k = \frac{g_{\text{r}(\text{F}_k)} - g_{\text{F}_k}^*}{g_{\text{r}(\text{F}_{k'})} + g_{\text{F}_k}^*}, \quad (22)$$

where $(k, k') = (1, 2)$ or $(2, 1)$. We emphasize that $g'_{\text{sd}(\text{F}_2)}(\mathbf{p})$, $g_{\text{F}_2}^*(\mathbf{p})$, $\lambda_2(\mathbf{p})$, and $\tilde{\sigma}_{E(\text{F}_2)}(\mathbf{p})$ depend on the direction of \mathbf{p} , according to their definition, Eqs. (10), (11), (15), (16), and (22). On the other hand, λ_1 is independent of \mathbf{m} because the F_1 layer does not show the anomalous Hall effect nor anisotropic magnetoresistance effect.

We assume that F_1 is a perpendicular magnet with an anisotropy field given by $\mathbf{H} = (0, 0, (H_K - M_s)m_z)$, where H_K is the perpendicular anisotropy field. In the absence of an electric field E_x , the free layer magnetization is stable along the perpendicular axis. We assume that it

starts along the z -axis, i.e., $\mathbf{m} = \hat{\mathbf{z}}$. In the presence of the spin torque, the magnetization is destabilized, and starts to precess around the z -axis. Assuming that $m_z \simeq 1$ and $|m_x|, |m_y| \ll 1$, we can linearize the LLG equation (see Appendix C) and determine the critical current

$$j_{\text{crit}} = - \frac{2\alpha\epsilon\mu_0 M_s d_1 (H_K - M_s)}{\hbar \tanh[d_2/(2\ell_{\text{sf}}^2)]} \times \frac{(1 - \lambda_1 \lambda_2 p_z^2)^2 g'_{\text{sd}(F_2)} (g_{\text{r}(F_1)} + g_{F_2}^*) \sigma_{F_2}}{(1 - \lambda_1 \lambda_2) p_z g_{F_2}^* g_{\text{r}(F_1)} \tilde{\sigma}_{E(F_2)}}. \quad (23)$$

Using Eq. (23), we can estimate the critical current for field-free switching of perpendicular layers. As an example, let us assume that F_2 has the anomalous Hall effect only, i.e., $\sigma_{\text{AH}(F_2)} \neq 0$ and $\sigma_{\text{AMR}(F_2)} = 0$. In this case, $\tilde{\sigma}_{E(F_2)}$ is $(\beta_{F_2} - \zeta_{F_2}) p_y \sigma_{\text{AH}(F_2)}$ and Eq. (23) can be simplified to Eq. (C3). We choose the pinned layer magnetization to be $\mathbf{p} = (0, 1/\sqrt{2}, 1/\sqrt{2})$ and take the parameter values given in Table I. For 10 nm of FePt, which can be fixed in a partially out of plane configuration, as a polarizer and 1 nm of CoFeB, with perpendicular anisotropy, as a free layer, we find a critical current of 1.0×10^{12} A/m² from Eq. (23). In Fig. 3, we show the magnetization dynamics obtained by numerically solving the LLG equation (20) for the electric current densities of (a) $j = 0.9 \times j_c$ and (b) $j = 1.5 \times j_c$, respectively. The magnetization stays near the initial direction in (a), whereas it switches the direction to $\mathbf{m} = -\hat{\mathbf{z}}$, showing the validity of Eq. (23).

Figure 4 shows the switching current as a function of the orientation of the fixed layer magnetization $\mathbf{p} = (\sin(\theta_{\text{fixed}}) \cos(\phi_{\text{fixed}}), \sin(\theta_{\text{fixed}}) \sin(\phi_{\text{fixed}}), \cos(\theta_{\text{fixed}}))$ from Eq. (23), and verified by numerical simulation of the LLG equation. The three panels show switching due to the anomalous Hall effect and anisotropic magnetoresistance separately and combined. For the parameters chosen here, given in Table I, the anomalous Hall effect is more efficient. The figure shows that the most efficient switching occurs when the polarizer magnetization is close to perpendicular ($\theta_{\text{fixed}} \approx 0^\circ$). The efficiency is determined by a competition between two effects. One effect is the efficiency of the spins at destabilizing the magnetization toward reversal. Spins injected perpendicular to the stable magnetization direction exert the greatest torque, but since they enhance precession only over half a period and suppress it over the other, they do not destabilize the magnetization. Electrons with moments antiparallel to the magnetization exert no torque, but when the magnetization fluctuates, they exert a torque that destabilizes the magnetization over the whole precession period. When the critical current is large enough, they overcome the damping and any fluctuations get magnified, leading to reversal. The counterbalancing effect is that when the pinned layer magnetization is collinear with the magnetization, it is also collinear with the film normal and the injected spin current goes to zero. So, the most efficient switching

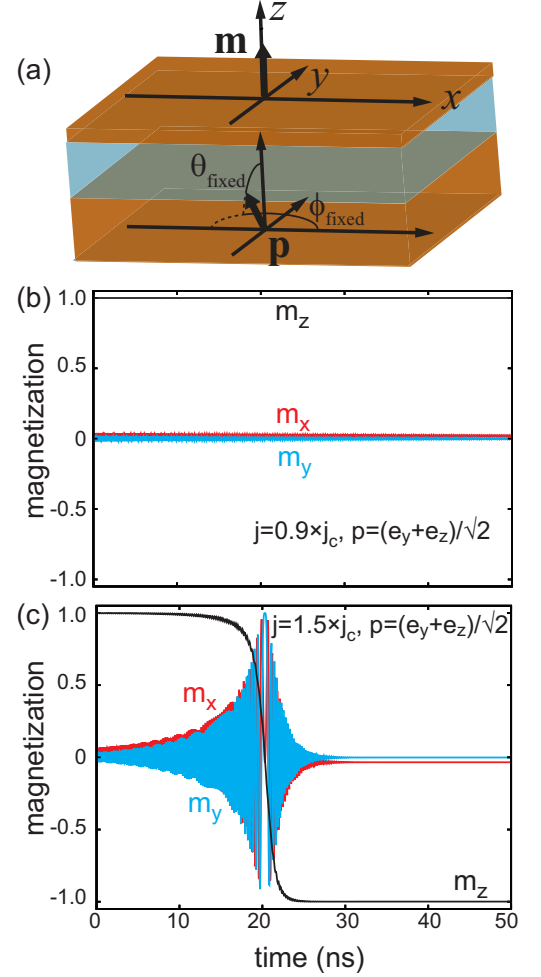


FIG. 3: (color online) Magnetization dynamics due to the anomalous Hall effect. Panel (a) shows the geometry. The trajectories obtained by numerically solving the LLG equation (20) are shown in (b) for $j = 0.9 \times j_c$ and (c) for $j = 1.5 \times j_c$.

occurs with the pinned layer magnetization close to normal but not all the way there, maximizing the total perpendicular component of the injected spins. Switching due to the anomalous Hall effect and that due to anisotropic magnetoresistance depend differently on the azimuthal angle so for some orientations of the fixed layer magnetization, they compete, but for others they cooperate to reduce the critical current.

The critical current is minimized at an optimal direction of \mathbf{p} . Because of complex dependences of $\tilde{\sigma}_E$ and $\tilde{\sigma}_{\delta\mu}$ on the magnetization direction, as shown in Eqs. (10) and (11), it is difficult to derive a formula of this optimal direction. However, for the F_2 with the anomalous Hall effect only, we can derive the analytical formula of the optimum direction of \mathbf{p} ; see Appendix C 1. The result, for this set of parameters is $\theta_{\text{fixed}} = 31.6^\circ$, $\phi_{\text{fixed}} = 90^\circ$.

We can compare these results with the magnetization switching assisted by the spin Hall effect. In the spin

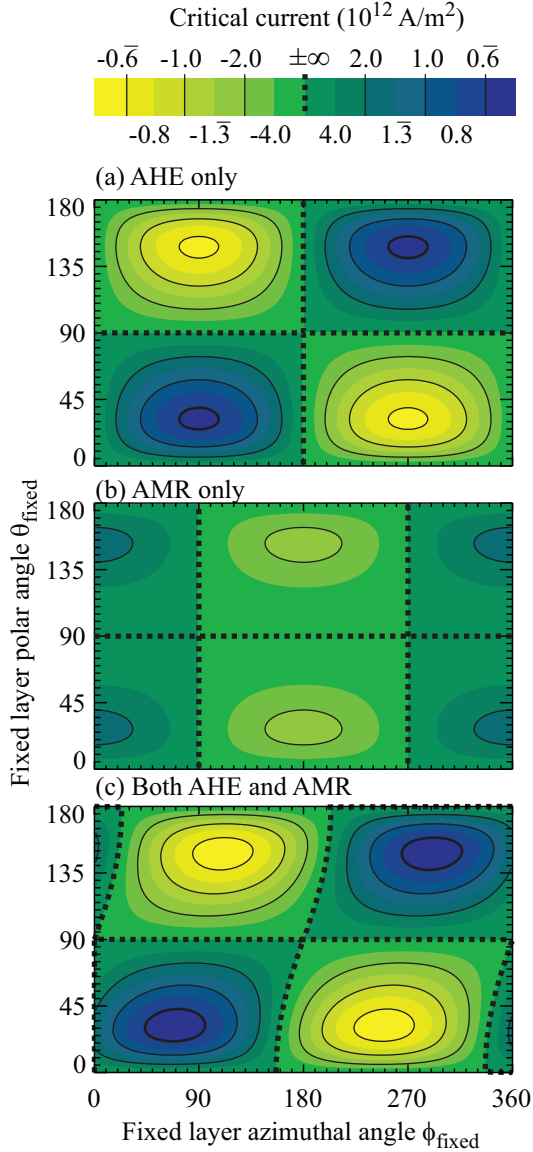


FIG. 4: (color online) Critical currents for a CoFeB free layer and FePt fixed layer as a function of the fixed layer magnetization direction. The contours are chosen uniformly in the inverse critical current, the contour where the critical currents diverge is labeled $\pm\infty$. In panel (a), we assume that the polarizer has anomalous Hall effect (AHE) but no anisotropic magnetoresistance (AMR). In panel (b), we assume it has the AMR but no AHE, and in panel (c) we assume it has both. Dark (blue) regions indicate regions with low critical for one direction of current flow and light (yellow) regions indicate low critical currents for the other direction. At the equator ($\theta_{\text{fixed}} = 90^\circ$), the critical currents diverge for all three cases, however, for the case with only AMR [panel (b)], the sign does not change as θ_{fixed} is varied near that point, but for the other two cases it does.

Hall effect, spin current polarized along the \hat{y} direction is injected to the free layer. This situation is similar to a special case of switching by spin-orbit effects in ferromagnets in which the pinned layer magnetization is in the \hat{y} direction. It is useful to consider a generalized situation with the fixed layer magnetization in the yz -plane, $\phi_{\text{fixed}} = 90^\circ$ with no anisotropic magnetoresistance. Then, $\tilde{\sigma}_E$ simplifies and Eq. (23) has the factor $p_y p_z$ in the denominator as seen in Eq. (C3). This factor implies that j_c^{AH} diverges when \mathbf{p} points to the z -direction ($p_y = 0$ and $p_z = 1$) because the anomalous Hall effect does not induce spin current along the z -direction when $p_y = 0$. The critical current also diverges when \mathbf{p} points to the y -direction ($p_y = 1$ and $p_z = 0$) because the spin-transfer torque never overcomes the damping torque as needed to enhance precession. This is the equivalent of switching by the spin Hall effect. While the spin-transfer torque can excite magnetization dynamics, when the fixed layer magnetization is along \hat{y} it does not overcome the damping and does not cause precession to become unstable.

It is possible to excite dynamics in perpendicularly magnetized samples with the spin Hall effect (or the anomalous Hall effect with $\mathbf{p} = \hat{y}$) as shown by Lee *et al.*²³. In fact, they demonstrate that it is possible to switch the magnetization. However, the switching they observe is not due to the spin transfer torque overcoming the damping, but rather is due to a large amplitude excitation due to the rapid onset of the current and hence torque. However, since nothing in the system breaks the symmetry between up and down, such switching is extremely sensitive to pulse duration and current amplitude. Lee *et al.*²³ demonstrate such sensitivity in Fig. 1(b) of their paper. They derive an analytic form, Eq. (5), for the critical current that is independent of the damping parameter. This independence indicates that the switching mechanism is precessional, rather than due to overcoming damping. To switch the magnetization direction without such sensitivity, an in-plane magnetic field slightly tilted to the z -direction has been used experimentally⁷⁷. The switching mechanism due to the anomalous Hall effect with a fixed layer with an out-of-plane component to the magnetization has the advantage of being largely independent of the current density or pulse duration for currents above the critical current. Another advantage is that the external field is unnecessary to switch the magnetization. It can also be significantly lower when the damping parameter is small, as is desirable in many magnetic devices.

C. Domain wall motion

The spin-orbit torques generated by ferromagnets can also be useful to displace in-plane magnetic domain walls, which we illustrate through two simple examples. We first consider the spin-valve illustrated in Fig. 5(a), with an in-plane domain wall in the free layer F1 and a uni-

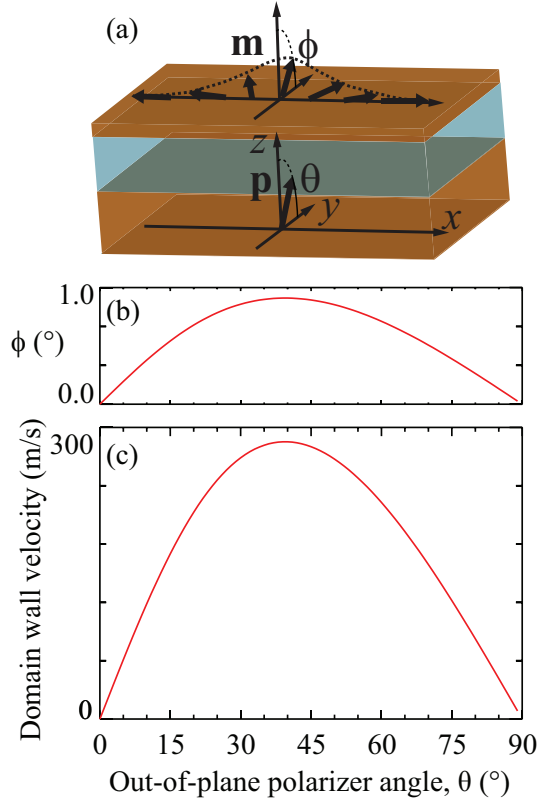


FIG. 5: (color online) (a) Schematic of the spin valve with a transverse in-plane wall and a fixed uniform polarizer. (b) Out-of-plane tilt angle of domain wall and (c) Domain wall velocity as a function of the out-of-plane angle θ of the polarizer. Calculations are done for 10 nm Py for a polarizer layer, 1 nm Py for a free layer, and a charge current density of 2×10^{11} A/m².

form polarizer $\mathbf{p} = (0, p_y, p_z)$ in the fixed layer F2. Due to the spin orbit effects in F2, a torque is generated on F1 that has the form : $\mathbf{T} = \tau_{so}(\mathbf{m}, \mathbf{p}) \mathbf{m} \times (\mathbf{m} \times \mathbf{p})$. To study the effect of this torque we consider a 1D model⁷⁸ of a transverse wall profile with a domain wall width Δ . The magnetization in the free layer, with the domain wall, is subject to a spin current from a fixed layer below. This spin current will cause a small tilting of the magnetization away from the long axis in all of the domains and will cause motion of the domain wall. We neglect the small tilting of the domains to get the following equations for the domain wall dynamics:

$$\dot{\phi} + \frac{\alpha}{\Delta} \dot{q} = \tau_{so} p_z \cos \phi - \tau_{so} p_y \sin \phi \quad (24)$$

$$\frac{\dot{q}}{\Delta} - \alpha \dot{\phi} = \gamma_0 H_k \sin \phi \cos \phi \quad (25)$$

Here q is the domain wall position, ϕ the out-of-plane tilt angle and H_k the shape anisotropy. At equilibrium in the absence of spin torques, ϕ is equal to zero and the domain wall lies in plane.

In the regime below Walker breakdown, the wall moves with a constant tilt angle and a steady velocity. Assuming the tilt is small, $\sin \phi \ll 1$,

$$\begin{aligned} \phi &= \frac{\tau_{so} p_z}{\alpha \gamma_0 H_k + \tau_{so} p_y} \\ \dot{q}_{AH} &= \frac{\Delta}{\alpha} \tau_{so} p_z \frac{\alpha \gamma_0 H_k}{\alpha \gamma_0 H_k + \tau_{so} p_y} \end{aligned} \quad (26)$$

Since $\alpha \gamma_0 H_k \gg \tau_{so}$ for typical values of the current density, the out-of-plane tilt is indeed small. The domain wall moves steadily only if the generated spin torque has a component along the z -direction. This is not the case of the torque generated by pure spin Hall effect in a non-magnetic heavy metal, in which case the domain wall does not move.⁷⁹ On the other hand, the spin-orbit torques generated by a ferromagnet can have components along both the z and y directions when the polarizer is tilted out-of-plane. If, as we did in the last section, we consider the case of the torque generated by just the anomalous Hall effect in F2, then

$$\begin{aligned} \tau_{AH} &= \frac{\gamma_0 \hbar}{2e\mu_0 M_s} \frac{\tanh[d_2/(2\ell_{sf})]}{d_1} \frac{g^* g_r}{g'_{sd}(g_r + g^*)} \\ &= \frac{1}{1 - \lambda^2(\mathbf{m} \cdot \mathbf{p})^2} (\beta - \zeta) \sigma_{AH} E_x p_y \end{aligned} \quad (27)$$

This behavior is shown in Fig. 5, in which we treat the motion for the case with the anomalous Hall effect and anisotropic magnetoresistance in both layers. However, since we assume the magnetization lies in the $y-z$ plane, the anisotropic magnetoresistance plays a negligible role. Fig. 5 shows a relatively large domain wall velocity for a modest charge current density of 2×10^{11} A/m² and a very small out of plane tilt of less than a degree.

In the proposed spin-valve system, the current flowing in the ferromagnet F_1 through the domain wall will also give rise to the more familiar (intralayer) adiabatic and non-adiabatic spin-transfer torques on the domain wall, these can enhance or oppose the effect of the spin-orbit torques. In comparison, the domain wall velocity induced by these intralayer torques is :

$$\dot{q}_{na} = \frac{1}{\alpha} \frac{\gamma_0 \hbar}{2e\mu_0 M_s} P \beta_{na} \sigma E_x \quad (28)$$

where $P \approx \beta$ is the current polarization and β_{na} the proportionality factor between the non-adiabatic and adiabatic torques. The ratio of the velocities is

$$\frac{\dot{q}_{AH}}{\dot{q}_{na}} \approx \frac{\Delta}{d_1} \frac{p_y p_z (\beta - \zeta) \sigma_{AH}}{P \beta_{na} \sigma} F, \quad (29)$$

where F is a series of factors (see Eq. (27) of order one. In a typical material as NiFe, both the anomalous spin hall angle and the non-adiabatic parameter β_{na} are close to 1 %⁵⁰. However, the domain wall will be mainly driven by the anomalous Hall torque because the wall width is typically much bigger than the layer thickness $\Delta/d > 10$

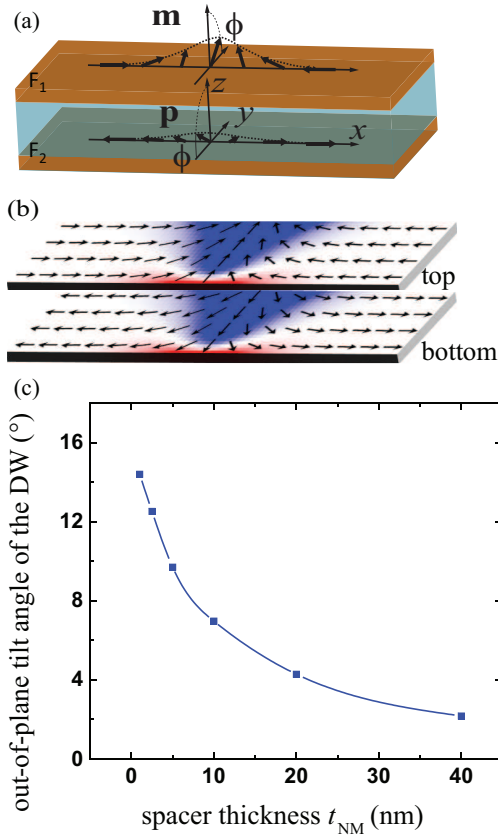


FIG. 6: (color on-line) (a) Schematic of the spin valve in anti-parallel configuration with two domain walls, one in each layer. (b) micromagnetic simulations of the coupled domain wall system showing in blue the positive z component of the magnetization. (c) Maximum out-of-plane tilt angle ϕ of the magnetization in the domain wall as a function of the spacer thickness.

for most systems.⁸⁰

The other system we consider is the coupled domain wall system shown in Fig. 6(a). In the case of a fixed polarizer F_2 and a free layer F_1 , F_2 can exert a torque on F_1 . But if F_2 is no longer fixed, F_1 can also induce a torque on F_2 . If the magnetic configuration is well chosen, these reciprocal torques can add and enhance magnetization dynamics of the coupled system. This is the case for the double domain wall system with anti-parallel configuration shown in Fig. 6.

If both magnetic layers are unpinned, the domain walls in each layer are strongly coupled. Domain walls in wires with opposite in-plane magnetizations tilt out of plane significantly due to the dipolar interaction between them, as shown in Fig. 6. In equilibrium, one domain wall has the out-of-plane tilt angle ϕ_0 , and the other $\pi - \phi_0$ so that the out-of-plane component is in the same direction and the in-plane directions are opposite. This configuration is illustrated in the micromagnetic simulations in Fig. 6(b) where blue shows the out-of-plane component of the magnetization.⁸¹ As the spacer thickness t_{NM} de-

creases, the dipolar fields on each domain wall increase, and the maximum out-of-plane tilt angle increases as shown in Fig. 6(b), reaching values close to 15° for spacer thicknesses typical of synthetic antiferromagnets.

In this configuration, the domain wall in F_2 polarizes the domain wall in F_1 (and reciprocally), and we can replace p_y and p_z respectively by $-\cos\phi$ and $\sin\phi$ in Eq. (24). For small angle deviations from the equilibrium configuration, this immediately leads to

$$\dot{q}_{AH} = \frac{\Delta}{\alpha} \tau_{so} \sin(2\phi_0) \quad (30)$$

Due to the particular symmetry of the anomalous Hall effect torques, the domain wall in F_2 acquires the same velocity: the motion of the coupled domain wall system is self-sustained. For small spacer thicknesses, the tilt angle is large, and velocities comparable to the single wall system with a uniform tilted fixed polarizer can be reached.

IV. SUMMARY

In this paper we develop a drift-diffusion approach to treat transport effects of spin-orbit coupling in ferromagnets. These include the anomalous Hall effect and the anisotropic magnetoresistance. In addition to the transverse charge currents that arise due to these effects, there are concomitant spin currents. These spin currents flow perpendicularly to the electric field, and so can be injected into layers perpendicular to the electrical current flow. When these other layers are ferromagnets with magnetizations that are not aligned with the original layer, they create spin transfer torques. Unlike the related spin Hall effect in non-magnetic materials, the ferromagnetic spin-orbit effects allow some control of the orientation of the injected spins. This control arises because the flowing spins in a ferromagnet are collinear with the magnetization. Changing the orientation of the magnetization changes the direction of the spins injected into other layers.

We compute the torques due to current flow for two ferromagnet layers separated by a thin non-magnetic layer. The control of the direction of the injected spins makes it possible to switch perpendicularly magnetized layers more easily because of the possibility of an out-of-plane component of the torque. We also show that such torques make it possible to switch in-plane magnetized layers via propagation of transverse/vortex walls and can efficiently induce dynamics in coupled magnetic systems, e.g. coupled transverse domain walls.

Acknowledgments

The authors thank Robert McMichael for useful discussions. JG acknowledges funding from the European

Appendix A: Solution of electro-chemical potential and spin accumulation

The x and z -components of Eq. (6) are explicitly given terms of $\bar{\mu}$ and $\delta\mu$ by

$$j_x = \sigma E_x + \frac{\sigma_{\text{AH}}}{e} (\partial_z \bar{\mu}) m_y + \sigma_{\text{AMR}} \left[E_x m_x + \frac{1}{e} (\partial_z \bar{\mu}) m_z \right] m_x + \zeta \frac{\sigma_{\text{AH}}}{e} (\partial_z \delta\mu) m_y + \eta \frac{\sigma_{\text{AMR}}}{e} (\partial_z \delta\mu) m_z m_x, \quad (\text{A1})$$

$$j_z = \frac{\sigma}{e} \partial_z \bar{\mu} - \sigma_{\text{AH}} E_x m_y + \sigma_{\text{AMR}} \left[E_x m_x + \frac{1}{e} (\partial_z \bar{\mu}) m_z \right] m_z + \beta \frac{\sigma}{e} \partial_z \delta\mu + \eta \frac{\sigma_{\text{AMR}}}{e} (\partial_z \delta\mu) m_z^2. \quad (\text{A2})$$

The continuity equation for electric current in steady state, $\nabla \cdot \mathbf{j} = \partial_z j_z = 0$, requires $(\sigma + \sigma_{\text{AMR}} m_z^2) \bar{\mu} + (\beta\sigma + \eta\sigma_{\text{AMR}} m_z^2) \delta\mu = Cz + D + F(x)$, where C and D are the integral constants whereas $F(x) \propto eE_x x$. The condition $j_z = 0$ implies $C = e(\sigma_{\text{AH}} m_z - \sigma_{\text{AMR}} m_z m_x) E_x$, whereas the other integral constant D corresponds to a shift of the chemical potential, μ_{shift} . Then, the electro-chemical potential is

$$\bar{\mu} = \mu_{\text{shift}} + eE_x x + \left(\frac{\sigma_{\text{AH}} m_y - \sigma_{\text{AMR}} m_z m_x}{\sigma + \sigma_{\text{AMR}} m_z^2} \right) eE_x z - \frac{1}{2} \left(\frac{\beta\sigma + \eta\sigma_{\text{AMR}} m_z^2}{\sigma + \sigma_{\text{AMR}} m_z^2} \right) (\mu^\uparrow - \mu^\downarrow). \quad (\text{A3})$$

We assume that the spin accumulation obeys the diffusion equation, Eq. (8). The solution can be expressed as $\mu^\uparrow - \mu^\downarrow = Ae^{z/\ell_{\text{sf}}} + Be^{-z/\ell_{\text{sf}}}$. Two integral constants, A and B , are determined as follows. Using Eq. (A3), the z -component of Eq. (7) is Eq. (9) and the spin current is $-\hbar/(2e)(j_z^\uparrow - j_z^\downarrow)$. When the ferromagnet lies in the region $0 \leq z \leq d$, and the spin current densities at $z = 0$ and d are given by $j_{sz}^{(1)}$ and $j_{sz}^{(2)}$, respectively, the integral constants, A and B are determined as

$$\frac{\tilde{\sigma}_{\delta\mu}}{2e\ell_{\text{sf}}} A = \frac{1}{2 \sinh(d/\ell_{\text{sf}})} \left[j_{sz}^{(1)} e^{-d/\ell_{\text{sf}}} - j_{sz}^{(2)} - \tilde{\sigma}_E (1 - e^{-d/\ell_{\text{sf}}}) E_x \right], \quad (\text{A4})$$

$$\frac{\tilde{\sigma}_{\delta\mu}}{2e\ell_{\text{sf}}} B = \frac{1}{2 \sinh(d/\ell_{\text{sf}})} \left[j_{sz}^{(1)} e^{d/\ell_{\text{sf}}} - j_{sz}^{(2)} + \tilde{\sigma}_E (e^{d/\ell_{\text{sf}}} - 1) E_x \right]. \quad (\text{A5})$$

These give Eq. (12). In the geometry shown in Fig. 1, the spin current at the F/N interface is $-\mathbf{m} \cdot \mathbf{Q}_s^{\text{F}_1 \rightarrow \text{N}}$ or $\mathbf{p} \cdot \mathbf{Q}_s^{\text{F}_2 \rightarrow \text{N}}$, and it is zero at the outer boundaries. Using these boundary conditions, Eq. (13) can be rewritten as Eq. (14). Note that $(j_z^\uparrow - j_z^\downarrow)$ satisfies

$$e \frac{\partial(j_z^\uparrow - j_z^\downarrow)}{\partial z} = \frac{(\sigma + \sigma_{\text{AMR}} m_z^2)^2 - (\beta\sigma + \eta\sigma_{\text{AMR}} m_z^2)^2}{(\sigma + \sigma_{\text{AMR}} m_z^2)} \frac{(\mu^\uparrow - \mu^\downarrow)}{2\ell_{\text{sf}}^2}, \quad (\text{A6})$$

which becomes $[e/(1 - \beta^2)\sigma] \partial(j_z^\uparrow - j_z^\downarrow)/\partial z = \delta\mu/\ell_{\text{sf}}^2$ in the absence of the AMR effect, reproducing the diffusion equation in Ref. 63.

Appendix B: Details of the Calculation

The spin current is calculated from Eqs. (14) and (17) by assuming the conservation of the spin current inside the N layer, i.e., $\mathbf{Q}_s^{\text{F}_1 \rightarrow \text{N}} + \mathbf{Q}_s^{\text{F}_2 \rightarrow \text{N}} = \mathbf{0}$. This condition leads to the following equations to determine the components of $\boldsymbol{\mu}_\text{N}$;

$$\mathbf{M} \begin{pmatrix} \mu_x \\ \mu_y \\ \mu_z \end{pmatrix} = -\frac{4\pi\hbar g_{\text{F}_2}^*(\mathbf{p})}{2eg'_{\text{sd}(\text{F}_2)}(\mathbf{p})} \tanh\left(\frac{d_2}{2\ell_{\text{sf}}^{\text{F}_2}}\right) \tilde{\sigma}_{E(\text{F}_2)}(\mathbf{p}) E_x S \begin{pmatrix} p_x \\ p_y \\ p_z \end{pmatrix} + \frac{4\pi\hbar g_{\text{F}_1}^*(\mathbf{m})}{2eg'_{\text{sd}(\text{F}_1)}(\mathbf{m})} \tanh\left(\frac{d_1}{2\ell_{\text{sf}}^{\text{F}_1}}\right) \tilde{\sigma}_{E(\text{F}_1)}(\mathbf{m}) E_x S \begin{pmatrix} m_x \\ m_y \\ m_z \end{pmatrix}. \quad (\text{B1})$$

Here, the components of the 3×3 matrix \mathbf{M} are given by

$$M_{1,1} = g_{F_1}^* m_x^2 + g_{r(F_1)} (1 - m_x^2) + g_{F_2}^* p_x^2 + g_{r(F_2)} (1 - p_x^2), \quad (B2)$$

$$M_{1,2} = (g_{F_1}^* - g_{r(F_1)}) m_x m_y + g_{i(F_1)} m_z + (g_{F_2}^* - g_{r(F_2)}) p_x p_y + g_{i(F_2)} p_z, \quad (B3)$$

$$M_{1,3} = (g_{F_1}^* - g_{r(F_1)}) m_z m_x - g_{i(F_1)} m_y + (g_{F_2}^* - g_{r(F_2)}) p_z p_x - g_{i(F_2)} p_y, \quad (B4)$$

$$M_{2,1} = (g_{F_1}^* - g_{r(F_1)}) m_x m_y - g_{i(F_1)} m_z + (g_{F_2}^* - g_{r(F_2)}) p_x p_y - g_{i(F_2)} p_z, \quad (B5)$$

$$M_{2,2} = g_{F_1}^* m_y^2 + g_{r(F_1)} (1 - m_y^2) + g_{F_2}^* p_y^2 + g_{r(F_2)} (1 - p_y^2), \quad (B6)$$

$$M_{2,3} = (g_{F_1}^* - g_{r(F_1)}) m_y m_z + g_{i(F_1)} m_x + (g_{F_2}^* - g_{r(F_2)}) p_y p_z + g_{i(F_2)} p_x, \quad (B7)$$

$$M_{3,1} = (g_{F_1}^* - g_{r(F_1)}) m_z m_x + g_{i(F_1)} m_y + (g_{F_2}^* - g_{r(F_2)}) p_z p_x + g_{i(F_2)} p_y, \quad (B8)$$

$$M_{3,2} = (g_{F_1}^* - g_{r(F_1)}) m_y m_z - g_{i(F_1)} m_x + (g_{F_2}^* - g_{r(F_2)}) p_y p_z - g_{i(F_2)} p_x, \quad (B9)$$

$$M_{3,3} = g_{F_1}^* m_z^2 + g_{r(F_1)} (1 - m_z^2) + g_{F_2}^* p_z^2 + g_{r(F_2)} (1 - p_z^2). \quad (B10)$$

The solution of $\boldsymbol{\mu}_N = (\mu_x, \mu_y, \mu_z)$ can be obtained by calculating the inverse of \mathbf{M} . In Eq. (B1), we added " \mathbf{p} " and " \mathbf{m} " after g^* , g'_{sd} , and $\tilde{\sigma}_E$ to emphasize that these quantities depend explicitly on the magnetization direction through Eqs. (10), (11), (15), and (16). From $\boldsymbol{\mu}$ we evaluate the spin currents, Eqs. (14) and (17). The LLG equations for \mathbf{m} and \mathbf{p} are, respectively, given by

$$\frac{d\mathbf{m}}{dt} = -\gamma_0 \mathbf{m} \times \mathbf{H} + \frac{\gamma_0}{\mu_0 M_s V} \mathbf{m} \times (\mathbf{Q}_s^{F_1 \rightarrow N} \times \mathbf{m}) + \alpha \mathbf{m} \times \frac{d\mathbf{m}}{dt}, \quad (B11)$$

$$\frac{d\mathbf{p}}{dt} = -\gamma_0 \mathbf{p} \times \mathbf{H} + \frac{\gamma_0}{\mu_0 M_s V} \mathbf{p} \times (\mathbf{Q}_s^{F_2 \rightarrow N} \times \mathbf{p}) + \alpha \mathbf{p} \times \frac{d\mathbf{p}}{dt}, \quad (B12)$$

where γ_0 and α are the gyromagnetic ratio and Gilbert damping constant, respectively. The volume is V .

1. Special cases for the spin torque

Although it is possible to solve Eq. (B1) analytically for an arbitrary magnetization alignment, the solution looks complicated. However, relatively simple analytical formulas can be obtained in some special cases. In this section, we discuss such cases. Note that Eq. (B1) comes from the conservation law for spin current inside the normal metal layer, $\mathbf{Q}_s^{F_1 \rightarrow N} + \mathbf{Q}_s^{F_2 \rightarrow N} = \mathbf{0}$, which can be written as

$$\begin{aligned} & g_{F_1}^* (\mathbf{m} \cdot \boldsymbol{\mu}_N) \mathbf{m} + g_{r(F_1)} \mathbf{m} \times (\boldsymbol{\mu}_N \times \mathbf{m}) + g_{i(F_1)} \boldsymbol{\mu}_N \times \mathbf{m} \\ & + g_{F_2}^* (\mathbf{p} \cdot \boldsymbol{\mu}_N) \mathbf{p} + g_{r(F_2)} \mathbf{p} \times (\boldsymbol{\mu}_N \times \mathbf{p}) + g_{i(F_2)} \boldsymbol{\mu}_N \times \mathbf{p} \\ & = s_1 \mathbf{m} - s_2 \mathbf{p}, \end{aligned} \quad (B13)$$

where $s_k = [4\pi\hbar g_{F_k}^* / (2eg'_{sd(F_k)})] \tanh[d_k / (2\ell_{sf}^k)] \tilde{\sigma}_{E(F_k)} E_x S$ ($k = 1, 2$): see Eq. (B1). We expand $\boldsymbol{\mu}_N$ as

$$\boldsymbol{\mu}_N = a_m \mathbf{m} + b_m \mathbf{m} \times \mathbf{p} + c_m \mathbf{m} \times (\mathbf{p} \times \mathbf{m}). \quad (B14)$$

Substituting this expression into Eq. (B13), and using the simplification $g_i = 0$, the coefficients a_m , b_m , and c_m are

$$a_m = \frac{[(g_{r(F_1)} + g_{F_2}^*) + (g_{r(F_2)} - g_{F_2}^*)(\mathbf{m} \cdot \mathbf{p})^2] s_1 - (g_{r(F_1)} + g_{r(F_2)}) \mathbf{m} \cdot \mathbf{p} s_2}{(g_{r(F_1)} + g_{F_2}^*)(g_{r(F_2)} + g_{F_1}^*) - (g_{r(F_1)} - g_{F_1}^*)(g_{r(F_2)} - g_{F_2}^*)(\mathbf{m} \cdot \mathbf{p})^2}, \quad (B15)$$

$$b_m = 0, \quad (B16)$$

$$c_m = \frac{(g_{r(F_2)} - g_{F_2}^*) \mathbf{m} \cdot \mathbf{p} s_1 - (g_{r(F_2)} + g_{F_1}^*) s_2}{(g_{r(F_1)} + g_{F_2}^*)(g_{r(F_2)} + g_{F_1}^*) - (g_{r(F_1)} - g_{F_1}^*)(g_{r(F_2)} - g_{F_2}^*)(\mathbf{m} \cdot \mathbf{p})^2}. \quad (B17)$$

The spin torque acting on the magnetization of the F_1 layer, \mathbf{m} , is $[\gamma_0 / (\mu_0 M_s V)] \mathbf{m} \times (\mathbf{Q}_s^{F_1 \rightarrow N} \times \mathbf{m}) = -[\gamma_0 g_r / (4\pi\mu_0 M_s V)] \mathbf{m} \times (\boldsymbol{\mu}_N \times \mathbf{m})$. Then, the coefficient c_m and its direction $\mathbf{m} \times (\mathbf{p} \times \mathbf{m})$ gives the spin torque. The

explicit form of the spin torque acting on \mathbf{m} is

$$\begin{aligned} \frac{d\mathbf{m}}{dt} = & \frac{\gamma_0 \hbar E_x}{2e\mu_0 M_1 d_1} g_{r(F_1)} \frac{\mathbf{m} \times (\mathbf{p} \times \mathbf{m})}{1 - \lambda_1(\mathbf{m})\lambda_2(\mathbf{p})(\mathbf{m} \cdot \mathbf{p})^2}, \\ & \times \left\{ \frac{g_{F_2}^*(\mathbf{p}) \tanh[d_2/(2\ell_{sf}^{F_2})] \tilde{\sigma}_{E(F_2)}(\mathbf{p})}{g'_{sd(F_2)}(\mathbf{p})[g_{r(F_1)} + g_{F_2}^*(\mathbf{p})]} - \lambda_2(\mathbf{p}) \frac{g_{F_1}^*(\mathbf{m}) \tanh[d_2/(2\ell_{sf}^{F_1})] \tilde{\sigma}_{E(F_1)}(\mathbf{m})}{g'_{sd(F_1)}(\mathbf{m})[g_{r(F_1)} + g_{F_2}^*(\mathbf{p})]} \mathbf{m} \cdot \mathbf{p} \right\} \end{aligned} \quad (B18)$$

where λ_k is defined by Eq. (22). Note that the conductance g^* and g'_{sd} , and therefore λ , depend on not only the material parameters but also the magnetization direction when the anisotropic magnetoresistance effect is finite; see Eqs. (11), (15), and (16). Also, $\tilde{\sigma}_E$ depends on the magnetization direction, as shown in Eq. (10). Therefore, we add " (\mathbf{m}) " or " (\mathbf{p}) " after $g_{F_k}^*$, $g_{sd(F_k)}$, $\tilde{\sigma}_{E(F_k)}$, and λ_k to emphasize the fact that these depend on the magnetization direction, \mathbf{m} or \mathbf{p} . Similarly, the spin torque acting on the magnetization of the F_2 layer is given by

$$\begin{aligned} \frac{d\mathbf{p}}{dt} = & -\frac{\gamma_0 \hbar E_x}{2e\mu_0 M_2 d_2} g_{r(F_2)} \frac{\mathbf{p} \times (\mathbf{m} \times \mathbf{p})}{1 - \lambda_1(\mathbf{m})\lambda_2(\mathbf{p})(\mathbf{m} \cdot \mathbf{p})^2}, \\ & \times \left\{ \frac{g_{F_1}^*(\mathbf{m}) \tanh[d_1/(2\ell_{sf}^{F_1})] \tilde{\sigma}_{E(F_1)}(\mathbf{m})}{g'_{sd(F_1)}(\mathbf{m})[g_{r(F_2)} + g_{F_1}^*(\mathbf{m})]} - \lambda_1(\mathbf{m}) \frac{g_{F_2}^*(\mathbf{p}) \tanh[d_2/(2\ell_{sf}^{F_2})] \tilde{\sigma}_{E(F_2)}(\mathbf{p})}{g'_{sd(F_2)}(\mathbf{p})[g_{r(F_2)} + g_{F_1}^*(\mathbf{m})]} \mathbf{m} \cdot \mathbf{p} \right\} \end{aligned} \quad (B19)$$

These formulas can be simplified in the absence of the anisotropic magnetoresistance effect, which we show in the following sections.

a. When $\sigma_{AMR} = 0$ and only the F_2 has an anomalous Hall effect

In the absence of the anisotropic magnetoresistance effect, i.e., $\sigma_{AMR} = 0$, g^* , g'_{sd} , and λ become independent from the magnetization directions. In this section, we also assume that the material parameters are identical between two ferromagnets, for simplicity. In this case, many of the derived parameters become independent of the layer and we suppress those indices.

Since $\tilde{\sigma}_E$ of the F_1 layer is zero and that of the F_2 layer is $\tilde{\sigma}_{E(F_2)} = (\beta - \zeta)\sigma_{AH}p_y$. The conductance g_{sd} , Eq. (16), and g^* , Eq. (15), are independent of the magnetization direction because $\tilde{\sigma}_{\delta\mu} = (1 - \beta^2)\sigma$ is independent of the magnetization direction. Then, from Eq. (B18), the spin torque acting on \mathbf{m} is

$$\frac{d\mathbf{m}}{dt} = \frac{\gamma_0 \hbar}{2eM_s d} \frac{g^* g_r (\beta - \zeta) \tanh[d/(2\ell_{sf})] \sigma_{AH} E_x}{g'_{sd} (g_r + g^*)} p_y \frac{\mathbf{m} \times (\mathbf{p} \times \mathbf{m})}{1 - \lambda^2 (\mathbf{m} \cdot \mathbf{p})^2}. \quad (B20)$$

Similarly, the spin torque acting on the F_2 layer, \mathbf{p} , is obtained from Eq. (B19) as

$$\frac{d\mathbf{p}}{dt} = \frac{\gamma_0 \hbar}{2e\mu_0 M_s d} \frac{g^* g_r (\beta - \zeta) \tanh[d/(2\ell_{sf})] \sigma_{AH} E_x}{g'_{sd} (g_r + g^*)} p_y \lambda \mathbf{m} \cdot \mathbf{p} \frac{\mathbf{p} \times (\mathbf{m} \times \mathbf{p})}{1 - \lambda^2 (\mathbf{m} \cdot \mathbf{p})^2}. \quad (B21)$$

b. When $\sigma_{AMR} = 0$ and both the F_1 and F_2 layers show the anomalous Hall effect

In this case, $\tilde{\sigma}_E$ of the F_1 and F_2 layers are given by $(\beta - \zeta)\sigma m_y$ and $(\beta - \zeta)\sigma p_y$, respectively. The spin torques acting on \mathbf{m} and \mathbf{p} are obtained from Eqs. (B18) and (B19) as

$$\frac{d\mathbf{m}}{dt} = \frac{\gamma_0 \hbar}{2e\mu_0 M_s d} \frac{g^* g_r (\beta - \zeta) \tanh[d/(2\ell_{sf})] \sigma_{AH} E_x}{g'_{sd} (g_r + g^*)} \left[\frac{p_y - m_y \lambda \mathbf{m} \cdot \mathbf{p}}{1 - \lambda^2 (\mathbf{m} \cdot \mathbf{p})^2} \right] \mathbf{m} \times (\mathbf{p} \times \mathbf{m}). \quad (B22)$$

$$\frac{d\mathbf{p}}{dt} = \frac{\gamma_0 \hbar}{2e\mu_0 M_s d} \frac{g^* g_r (\beta - \zeta) \tanh[d/(2\ell_{sf})] \sigma_{AH} E_x}{g'_{sd} (g_r + g^*)} \left[\frac{p_y \lambda \mathbf{m} \cdot \mathbf{p} - m_y}{1 - \lambda^2 (\mathbf{m} \cdot \mathbf{p})^2} \right] \mathbf{p} \times (\mathbf{m} \times \mathbf{p}). \quad (B23)$$

Appendix C: Linearized LLG equation

Linearizing the LLG equation, Eq. (20) gives

$$\frac{1}{\gamma_0} \frac{d}{dt} \begin{pmatrix} m_x \\ m_y \end{pmatrix} + \mathbf{C} \begin{pmatrix} m_x \\ m_y \end{pmatrix} = \frac{\hbar \tanh[d_2/(2\ell_{\text{sf}}^2)] E_x}{2e\mu_0 M_s d_1} \frac{g_{\text{F}_2}^* g_{\text{r}(\text{F}_1)} \tilde{\sigma}_{E(\text{F}_2)}}{g'_{\text{sd}(\text{F}_2)} (g_{\text{r}(\text{F}_1)} + g_{\text{F}_2}^*)} \frac{1}{1 - \lambda_1 \lambda_2 p_z^2} \begin{pmatrix} p_x \\ p_y \end{pmatrix}. \quad (\text{C1})$$

The coefficient matrix \mathbf{C} is given by

$$\mathbf{C} = \begin{pmatrix} \alpha(H_K - M_s) & (H_K - M_s) \\ -(H_K - M_s) & \alpha(H_K - M_s) \end{pmatrix} + \frac{\hbar \tanh[d_2/(2\ell_{\text{sf}}^2)] E_x}{2e\mu_0 M_s d_1} \frac{g_{\text{F}_2}^* g_{\text{r}(\text{F}_1)} \tilde{\sigma}_{E(\text{F}_2)}}{g'_{\text{sd}(\text{F}_2)} (g_{\text{r}(\text{F}_1)} + g_{\text{F}_2}^*)} \begin{pmatrix} \frac{[1 - \lambda_1 \lambda_2 (p_z^2 + 2p_x^2)] p_z}{(1 - \lambda_1 \lambda_2 p_z^2)^2} & -\frac{2\lambda_1 \lambda_2 p_x p_y p_z}{(1 - \lambda_1 \lambda_2 p_z^2)^2} \\ -\frac{2\lambda_1 \lambda_2 p_x p_y p_z}{(1 - \lambda_1 \lambda_2 p_z^2)^2} & \frac{[1 - \lambda_1 \lambda_2 (p_z^2 + 2p_y^2)] p_z}{(1 - \lambda_1 \lambda_2 p_z^2)^2} \end{pmatrix}. \quad (\text{C2})$$

The solutions of Eq. (C1) can be expressed as superpositions of $\exp\{\gamma_0[\pm i\sqrt{\det[\mathbf{C}] - (\text{Tr}[\mathbf{C}]/2)^2} - \text{Tr}[\mathbf{C}]/2]t\}$. When the real part of the exponent ($\propto -\gamma_0 \text{Tr}[\mathbf{C}]t$) is positive (negative), the amplitude of m_x and m_y increases (decreases) with time. Then, we define the critical electric field to excite the magnetization dynamics by the condition $\text{Tr}[\mathbf{C}] = 0$. In terms of the current density $j = \sigma E_x$, the critical current density is given by Eq. (23).

1. Optimum direction of \mathbf{p} to minimize Eq. (23)

When the polarizing layer has only the anomalous Hall effect and no anisotropic magnetoresistance, the critical current, Eq. (23) becomes

$$j_{\text{crit}}^{\text{AH}} = -\frac{2\alpha e\mu_0 M_s d_1 (H_K - M_s)}{\hbar \tanh[d_2/(2\ell_{\text{sf}}^2)]} \times \frac{(1 - \lambda_1 \lambda_2 p_z^2)^2 g'_{\text{sd}(\text{F}_2)} (g_{\text{r}(\text{F}_1)} + g_{\text{F}_2}^*) \sigma_{\text{F}_2}}{(\beta_{\text{F}_2} - \zeta_{\text{F}_2}) (1 - \lambda_1 \lambda_2) p_y p_z g_{\text{F}_2}^* g_{\text{r}(\text{F}_1)} \sigma_{\text{AH}(\text{F}_2)}}. \quad (\text{C3})$$

This is proportional to

$$j_{\text{crit}}^{\text{AH}} \propto \frac{(1 - \lambda_1 \lambda_2 p_z^2)^2}{p_y p_z}, \quad (\text{C4})$$

where λ_k is independent of the magnetization direction in this case. Then, $j_{\text{crit}}^{\text{AH}}$ is minimized when the polar angle θ_{fixed} is given by

$$\theta_{\text{fixed}} = \tan^{-1} \left[\sqrt{\frac{\lambda_1 \lambda_2 + 2 - \sqrt{(3\lambda_1 \lambda_2 - 2)^2 + 8\lambda_1 \lambda_2}}{3\lambda_1 \lambda_2 - 2 + \sqrt{(3\lambda_1 \lambda_2 - 2)^2 + 8\lambda_1 \lambda_2}}} \right]. \quad (\text{C5})$$

For the parameters shown in Fig. 4, the optimum angle is estimated to be $\theta_{\text{fixed}} = 31.6^\circ$.

¹ L. Berger, J. Appl. Phys. **55**, 1954 (1984) doi:10.1063/1.333530.

² J. Slonczewski, J. Magn. Magn. Mat. **159**, L1, (1996) doi:10.1016/0304-8853(96)00062-5.

³ L. Berger, Phys. Rev. B **54**, 9353 (1996) doi:10.1103/PhysRevB.54.9353.

⁴ M. D. Stiles and J. Miltat, Top. Appl. Phys. **101**, 225 (2006) doi:10.1007/10938171_7.

⁵ D. C. Ralph and M. D. Stiles, J. Magn. Magn. Mater. **320**, 1190 (2007) doi:10.1016/j.jmmm.2007.12.019.

⁶ K. Ando, S. Takahashi, K. Harii, K. Sasage, J. Ieda, S. Maekawa, and E. Saitoh, Phys. Rev. Lett. **101**, 036601 (2008) doi:10.1103/PhysRevLett.101.036601.

⁷ L. Liu, T. Moriyama, D. C. Ralph and R. A. Buhrman, Phys. Rev. Lett. **106**, 036601 (2011) doi:10.1103/PhysRevLett.106.036601.

⁸ M. I. Dyakonov and V. I. Perel, Sov. Phys. JETP Lett. **13** 467 (1971) Bibcode:1971JETPL..13..467D;

⁹ J. E. Hirsch, Phys. Rev. Lett. **83** 1834 (1999) doi:10.1103/PhysRevLett.83.1834;

- ¹⁰ S. Zhang, Phys. Rev. Lett. **85**, 393 (2000) doi:10.1103/PhysRevLett.85.393.
- ¹¹ Yu. A. Bychkov and E. I. Rashba, JETP. Lett. **39**, 78 (1984).
- ¹² V. M. Edelstein, Solid State Commun. **73**, 233 (1990) doi:10.1016/0038-1098(90)90963-C.
- ¹³ K. Obata, and G. Tatara, Phys Rev. B **77**, 214429 (2008) doi:10.1103/PhysRevB.77.214429.
- ¹⁴ A. Manchon and S. Zhang, Phys. Rev. B **78**, 212405 (2008) doi:10.1103/PhysRevB.78.212405.
- ¹⁵ A. Matos-Abiague and R. L. Rodriguez-Suarez, Phys. Rev. B **80**, 094424 (2009) doi:10.1103/PhysRevB.80.094424.
- ¹⁶ X. Wang and A. Manchon, Phys. Rev. Lett. **108**, 117201 (2012) doi:10.1103/PhysRevLett.108.117201.
- ¹⁷ K.-W. Kim, S.-M. Seo, J. Ryu, K.-J. Lee, and H.-W. Lee, Phys. Rev. B **85**, 180404(R) (2012) doi:10.1103/PhysRevB.85.180404.
- ¹⁸ D. A. Pesin and A. H. MacDonald, Phys. Rev. B **86**, 014416 (2012) doi:10.1103/PhysRevB.86.014416.
- ¹⁹ E. van der Bijl and R. A. Duine, Phys. Rev. B **86**, 094406 (2012) doi:10.1103/PhysRevB.86.094406.
- ²⁰ I. M. Miron, K. Garello, G. Gaudin, P.-J. Zermatten, M. V. Costache, S. Auffret, S. Bandiera, B. Rodmacq, A. Schuhl, and P. Gambardella, Nature (London) **476**, 189 (2011) doi:10.1038/nmat3020.
- ²¹ L. Liu, C.-F. Pai, Y. Li, H. W. Tseng, D. C. Ralph and R. A. Buhrman, Science **4**, 555 (2012) doi:10.1126/science.1218197.
- ²² K. Garello, C. O. Avci, I. M. Miron, O. Boulle, S. Auffret, P. Gambardella, and G. Gaudin, arXiv:1310.5586.
- ²³ K.-S. Lee, S.-W. Lee, B.-C. Min, and K.-J. Lee, Appl. Phys. Lett. **102**, 112410 (2013) doi:10.1063/1.4798288.
- ²⁴ K.-S. Lee, S.-W. Lee, B.-C. Min, and K.-J. Lee, Appl. Phys. Lett. **104**, 072413 (2014) doi:10.1063/1.4866186.
- ²⁵ I. M. Miron, T. Moore, H. Szambolics, L. D. Buda-Prejbeanu, S. Auffret, B. Rodmacq, S. Pizzini, J. Vogel, M. Bonfim, A. Schuhl, and G. Gaudin, Nat. Mater. **10**, 419 (2011) doi:10.1038/nmat3020.
- ²⁶ P. P. J. Haazen, E. Muré, J. H. Franken, R. Lavrijsen, H. J. M. Swagten, and B. Koopmans, Nat. Mater. **12**, 299 (2013) doi:10.1038/nmat3553.
- ²⁷ S. Emori, U. Bauer, S.-M. Ahn, E. Martinez, and G. S. D. Beach, Nat. Mater. **12**, 611 (2013) doi:10.1038/nmat3675.
- ²⁸ K.-S. Ryu, L. Thomas, S.-H. Yang, and S. S. P. Parkin, Nat. Nanotech. **8**, 527 (2013) doi:10.1038/nnano.2013.102.
- ²⁹ Y. Yoshimura, T. Koyama, D. Chiba, Y. Nakatani, S. Fukami, M. Yamanouchi, H. Ohno, K.-J. Kim, T. Moriyama, and T. Ono, Appl. Phys. Express **7**, 033005 (2014).
- ³⁰ S.-M. Seo, K.-W. Kim, J. Ryu, H.-W. Lee, and K.-J. Lee, Appl. Phys. Lett. **101**, 022405 (2012) doi:10.1063/1.4733674.
- ³¹ A. Thiaville, S. Rohart, É. Jué, V. Cros, and A. Fert, Europhys. Lett. **100**, 57002 (2012) doi:10.1209/0295-5075/100/57002.
- ³² J. Kim, J. Sinha, M. Hayashi, M. Yamanouchi, S. Fukami, T. Suzuki, S. Mitani, and H. Ohno, Nat. Mater. **12**, 240 (2013) doi:10.1038/nmat3522.
- ³³ X. Qiu, K. Narayanapillai, Y. Wu, P. Deorani, X. Yin, A. Rusydi, K.-J. Lee, H.-W. Lee, and H. Yang, arXiv:1311.3032.
- ³⁴ X. Fan, H. Celik, J. Wu, C. Ni, K.-J. Lee, V. O. Lorenz, and J. Q. Xiao, Nat. Commun. **5** 3042 (2014) doi:10.1038/ncomms4042.
- ³⁵ R. H. Liu, W. L. Lim, and S. Urazhdin, Phys. Rev. B **89**, 220409(R) (2014) doi:10.1103/PhysRevB.89.220409.
- ³⁶ K. Garello, I. M. Miron, C. O. Avci, F. Freimuth, Y. Mokrousov, S. Blügel, S. Auffret, O. Boulle, G. Gaudin, and P. Gambardella, Nat. Nanotech. **8**, 587 (2013) doi:10.1038/nnano.2013.145.
- ³⁷ X. Qiu, P. Deorani, K. Narayanapillai, K.-S. Lee, K.-J. Lee, H.-W. Lee, and H. Yang, Sci. Rep. **4**, 4491 (2014) doi:10.1038/srep04491.
- ³⁸ P. M. Haney, H.-W. Lee, K.-J. Lee, A. Manchon, and M. D. Stiles, Phys. Rev. B **87**, 174411 (2013) doi:10.1103/PhysRevB.87.174411.
- ³⁹ P. M. Haney, H.-W. Lee, K.-J. Lee, A. Manchon, and M. D. Stiles, Phys. Rev. B **88**, 214417 (2013) doi:10.1103/PhysRevB.88.214417.
- ⁴⁰ F. Freimuth, S. Blügel, Y. Mokrousov, arXiv:1305.4873.
- ⁴¹ F. Freimuth, S. Blügel, Y. Mokrousov, J. Phys. Condens. Matter **26**, 104202 (2014) doi:10.1088/0953-8984/26/10/104202.
- ⁴² H. Kurebayashi, J. Sinova, D. Fang, A. C. Irvine, T. D. Skinner, J. Wunderlich, V. Novák, R. P. Campion, B. L. Gallagher, E. K. Vehstedt, L. P. Zarobo, K. Vyborny, A. J. Ferguson, and T. Jungwirth, Nat. Nanotech. **9**, 211 (2014) doi:10.1038/nnano.2014.15.
- ⁴³ W. Thomson, Proc. Royal Soc. London **8** 546 (1857) doi:10.1098/rspl.1856.0144.
- ⁴⁴ T. McGuire and R. Potter, IEEE Trans. Magn. **11** 1018 (1975) doi:10.1109/TMAG.1975.1058782.
- ⁴⁵ A. Kundt, Ann. Phys. **285**, 257 (1893) doi:10.1002/andp.18932850603.
- ⁴⁶ E. M. Pugh and N. Rostoker, Rev. Mod. Phys. **25**, 151 (1953) doi:10.1103/RevModPhys.25.151.
- ⁴⁷ R. Karplus and J. M. Luttinger, Phys. Rev. **95** 1154 (1954) doi:10.1103/PhysRev.95.1154;
- ⁴⁸ N. A. Sinitsyn, J. Phys.: Condens. Matter **20** 023201 (2008) doi:10.1088/0953-8984/20/02/023201
- ⁴⁹ Naoto Nagaosa, Jairo Sinova, Shigeki Onoda, A. H. MacDonald, and N. P. Ong, Rev. Mod. Phys. **82**, 1539 (2010) doi:10.1103/RevModPhys.82.1539.
- ⁵⁰ B. F. Miao, S. Y. Huang, D. Qu, and C. L. Chien, Phys. Rev. Lett. **111**, 066602 (2013) doi:10.1103/PhysRevLett.111.066602.
- ⁵¹ A. Azevedo, O. Alves Santos, R. O. Cunha, R. Rodriguez-Suarez and S. M. Rezende Appl. Phys. Lett. **104**, 152408 (2014); doi:10.1063/1.4871514.
- ⁵² H. Wang, C. Du, P. C. Hammel, and F. Yang, Appl. Phys. Lett. **104**, 020405 (2014), doi:10.1063/1.4878540.
- ⁵³ A. Tsukahara, Y. Ando, Y. Kitamura, H. Emoto, E. Shikoh, M. P. Delmo, T. Shinjo, and M. Shiraishi, Phys. Rev. B **89**, 235317 (2014), doi:10.1103/PhysRevB.89.235317.
- ⁵⁴ M. Weiler, J. M. Shaw, H. T. Nembach, and T. J. Silva, Magn. Lett. In Press (2014) doi:10.1109/LMAG.2014.2361791.
- ⁵⁵ G. Y. Guo, S. Murakami, T. W. Chen, N. Nagaosa, Phys. Rev. Lett. **100**, 096401 (2008) doi:10.1103/PhysRevLett.100.096401
- ⁵⁶ T. Tanaka, H. Kontani, M. Naito, T. Naito, D. S. Hirashima, K. Yamada, and J. Inoue, Phys. Rev. B **77**, 165117 (2008) doi:10.1103/PhysRevB.77.165117.
- ⁵⁷ M. Gradhand, D. V. Fedorov, P. Zahn, and I. Mertig, Phys. Rev. Lett. **104**, 186403 (2010) doi:10.1103/PhysRevLett.104.186403.

- ⁵⁸ S. Lowitzer, M. Gradhand, D. Ködderitzsch, D. V. Fedorov, I. Mertig, and H. Ebert, Phys. Rev. Lett. **106**, 056601 (2011) DOI:10.1103/PhysRevLett.106.056601.
- ⁵⁹ A. Brataas, Y. V. Nazalov, and G. E. W. Bauer, Eur. Phys. J. B, **22**, p. 99 (2001) doi: 10.1007/PL00011139.
- ⁶⁰ A. Brataas, G. E. W. Bauer, and P. J. Kelly, Phys. Rep., **427**, p. 157 (2006) doi: 10.1016/j.physrep.2006.01.001.
- ⁶¹ Y. Tserkovnyak, A. Brataas, G. E. W. Bauer, and B. I. Halperin, Rev. Mod. Phys. **77**, p. 1375 (2005) doi: 10.1103/RevModPhys.77.1375.
- ⁶² Y. Mokrousov, B. Zimmermann, P. Mavropoulos, N. H. Long (Private Communication).
- ⁶³ T. Valet and A. Fert, Phys. Rev. B, **48**, p. 7099 (1993) doi:10.1103/PhysRevB.48.7099.
- ⁶⁴ R. E. Camley and J. Barnaś, Phys. Rev. Lett. **63**, 664 (1989) doi:10.1103/PhysRevLett.63.664.
- ⁶⁵ J. Bass and W. P. Pratt, J. Magn. Magn. Mater., **200**, 274 (1999) doi:10.1016/S0304-8853(99)00316-9.
- ⁶⁶ H. Oshima, K. Nagasaka, Y. Seyama, Y. Shimizu, S. Eguchi and A. Tanaka J. Appl. Phys. **91**, 8105 (2002); doi:10.1063/1.1448310
- ⁶⁷ J. Moritz, B. Rodmacq, S. Auffret and B. Dieny, J. Phys. D: Appl. Phys. **41** 135001 (2008) doi:10.1088/0022-3727/41/13/135001.
- ⁶⁸ T. Seki, Y. Hasegawa, S. Mitani, S. Takahashi, H. Imaura, S. Maekawa, J. Nitta and K. Takanashi, Nature Materials **7**, 125 (2008) doi:10.1038/nmat2098.
- ⁶⁹ G. E. W. Bauer, Y. Tserkovnyak, D. Huertas-Hernando, and A. Brataas, Adv. in Solid State Phys. **43**, 383 (2003) doi:10.1007/978-3-540-44838-9_27.
- ⁷⁰ C. Ahn, K.-H. Shin and W. P. Pratt Jr., Appl. Phys. Lett. **92**, 102509 (2008); <http://dx.doi.org/10.1063/1.2891065>
- ⁷¹ Y. Q. Zhang, N. Y. Sun, R. Shan, J. W. Zhang, S. M. Zhou, Z. Shi and G. Y. Guo J. Appl. Phys. **114**, 163714 (2013); doi:10.1063/1.4827198.
- ⁷² Th. G. S. M. Rijks, S. K. J. Lenczowski, R. Coehoorn, and W. J. M. de Jonge Phys. Rev. B **56**, 362 (1997) doi:10.1103/PhysRevB.56.362.
- ⁷³ C. Christides, I. Panagiotopoulos, D. Niarchos, T. Tsakalakos and A. F. Jankowski, J. Phys.: Condens. Matter **6** 8187 (1994) doi:10.1088/0953-8984/6/40/010.
- ⁷⁴ P. E. Tannenwald and M. H. Seavey, Jr. Phys. Rev. **105**, 377 (1957) doi:10.1103/PhysRev.105.377.
- ⁷⁵ Y. Zhang, W. Zhao, Y. Lakys, J.-O. Klein, J.-V. Kim, D. Ravelosona, and C. Chappert, IEEE Trans. Elect. Dev. **59**, 819 (2012) doi:10.1109/TED.2011.2178416.
- ⁷⁶ Y. Zhou, C. L. Zha, S. Bonetti, J. Persson and J. Åkerman, Appl. Phys. Lett. **92**, 262508 (2008); doi:10.1063/1.2955831.
- ⁷⁷ L. Liu, O. J. Lee, T. J. Gudmundsen, D. C. Ralph, and R. A. Buhrman, Phys. Rev. Lett. **109**, 096602 (2012) doi:10.1103/PhysRevLett.109.096602
- ⁷⁸ N. L. Schryer and L. R. Walker, J. Appl. Phys. **45**, 5406 (1974) doi:10.1063/1.1663252.
- ⁷⁹ A. V. Khvalkovskiy, V. Cros, D. Apalkov, V. Nikitin, M. Krounbi, K. A. Zvezdin, A. Anane, J. Grollier, and A. Fert, Phys. Rev. B **87**, 020402(R) (2013) doi:10.1103/PhysRevB.87.020402.
- ⁸⁰ P. J. Metaxas, J. Sampaio, A. Chanthbouala, R. Matsumoto, A. Anane, A. Fert, K. A. Zvezdin, K. Yakushiji, H. Kubota, A. Fukushima, S. Yuasa, K. Nishimura, Y. Nagamine, H. Maehara, K. Tsunekawa, V. Cros, J. Grollier, Sci Rep. **3**, 1829 (2013) doi:10.1038/srep01829.
- ⁸¹ Micromagnetic simulations using the open source software OOMMF⁸² with the following geometry: width 100 nm, length 2 μ m, thickness 5 nm, cell size 5 nm \times 5 nm \times 5 nm, micromagnetic exchange $A = 13.0$ pJ/m, and other materials parameters as in Table I.
- ⁸² M. J. Donahue and D. G. Porter, in *Interagency Report NISTIR 6376* (National Institute of Standards and Technology, Gaithersburg, MD, 1999).